



**CHALMERS**  
UNIVERSITY OF TECHNOLOGY

---



# **Suspension and Chassis Parameters Impact on Vehicle Handling and Road Holding**

Tool development for predicting the vehicle understeer

Master's Thesis in Automotive Engineering

Sumukh Kumble & Aditya Mukherjee



MASTER'S THESIS 2019:18

# **Suspension and Chassis Parameters Impact on Vehicle Handling and Road Holding**

Tool development for predicting the vehicle understeer

SUMUKH KUMBLE  
ADITYA MUKHERJEE



Department of Mechanics and Maritime Sciences  
Division of Vehicle Engineering and Autonomous Systems  
CHALMERS UNIVERSITY OF TECHNOLOGY  
Gothenburg, Sweden 2019

Suspension and Chassis Parameters Impact on Vehicle Handling and Road Holding  
- Tool development for predicting the vehicle understeer  
SUMUKH KUMBLE  
ADITYA MUKHERJEE

© SUMUKH KUMBLE & ADITYA MUKHERJEE, 2019.

Supervisor: Peter Folkow, Department of Mechanics and Maritime Sciences  
Examiner: Mathias Lidberg, Department of Mechanics and Maritime Sciences

Master's Thesis 2019:18  
Department of Mechanics and Maritime Sciences  
Division of Vehicle Engineering and Autonomous Systems  
Chalmers University of Technology  
SE-412 96 Gothenburg  
Telephone +46 31 772 1000

Cover: Steady State Cornering test at AstaZero, Courtesy of the student blog -  
"Study in Sweden".

Typeset in L<sup>A</sup>T<sub>E</sub>X  
Printed by Chalmers Reproservice  
Gothenburg, Sweden 2019

Suspension and Chassis Parameters Impact on Vehicle Handling and Road Holding  
Tool development for predicting vehicle understeer  
SUMUKH KUMBLE & ADITYA MUKHERJEE  
Department of Mechanics and Maritime Sciences  
Chalmers University of Technology

## Abstract

When developing suspension subsystems for a vehicle, it is necessary to be able to prepare the design for proper vehicle directional control and handling. A slight understeer behaviour is targeted at different driving conditions for a passenger vehicle and several suspension factors impact this behaviour of the vehicle. This thesis aims at understanding the effect of various suspension and chassis parameters on vehicle handling and development of a tool that predicts the vehicle steady state handling behaviour for a user defined suspension setup.

The tool is developed based on the slip angle definition of understeer and a handling diagram is generated as a result. The slip angles for the tires are determined by solving a set of non linear equations that describe the equations of motion. The tool is validated with experimental data from two different sources. The results of the tool match with the experimental data which validates the method and the tool developed.

The user interface for the tool is made simple to use. Various configurations for the suspension setup can be fed to the tool as an excel sheet and the results can be obtained by running a MATLAB code in the background.

Keywords: understeer, suspension, chassis, slip angle, handling, directional control, steady state cornering.



# Acknowledgements

The successful completion of any project involves a tremendous amount of support and backing up from the guides and well wishers. Unlike any other project, this master thesis would be incomplete without the mention of the people who made it possible by providing continued support and constant motivation and encouragement throughout this thesis.

Firstly, we would like to thank the department of Mechanical and Maritime Sciences, Chalmers University of Technology for providing an opportunity to work with this thesis. We are extremely grateful for the continuous support and encouragement from and our supervisors Prof. Mathias Lidberg and Prof. Peter Folkow through the entire project.

We are equally thankful to ÅF Industry AB for allowing us to work with them on this exciting and challenging master thesis. This thesis would not have been possible without the limitless and round the clock support of our supervisors Gunnar Olsson, Christoffer Routledge and Stefan Karlström.

Our sincere thanks to Gunnar Olsson, who has been of paramount importance from the very first day of the project. The rich and enlightening guidance of Gunnar is probably the most important factor for the success of this thesis. The discussions we had with Gunnar post our weekly meetings was a rich source of understanding the concepts of Vehicle Dynamics and a major support for the thesis.

We also take this opportunity to thank Christoffer Routledge for being an inspiration throughout the thesis. The suggestions by Christoffer provided a major direction for the development of the tool and the information we received from him has been enormous. The discussions with Christoffer was a source of new encouragement and a thrusting force to excel in the thesis. Our sincere thanks to him.

No project can be completed successfully without good project management. This thesis would not have been completed in time without the expert support of Stefan Karlström and we take this opportunity to thank him for his complete support and for not giving up on us. We will ever remember the 5-Cs of project management Stefan taught us and without Stefan, the project would not have been what it is now. We learnt a great amount of self management techniques from Stefan and he was an inspiration all the way until the end. Thank you Stefan for your most valued support.

Last but not the least, we would like to express our gratitude for friends and family for being there for us in the hard times during this thesis and filling us with confidence and motivation when we needed it the most. We like to thank everyone again for making this wonderful journey a success.

Sumukh Kumble & Aditya Mukherjee, Gothenburg, September 2019





# Contents

<b>List of Figures</b>	<b>xi</b>
<b>List of Tables</b>	<b>1</b>
<b>1 Introduction</b>	<b>1</b>
1.1 Background . . . . .	1
1.2 The Importance of Understeer . . . . .	1
1.3 Purpose . . . . .	2
1.4 Objective and the scope of the Thesis . . . . .	2
1.5 Delimitations . . . . .	2
<b>2 Vehicle System Modelling</b>	<b>3</b>
2.1 Vehicle Model and Equations of Motion . . . . .	3
2.1.1 The Two Track Vehicle Model . . . . .	3
2.1.2 Lateral Load Transfer . . . . .	5
2.2 The Tire . . . . .	7
2.2.1 Slip Angle . . . . .	7
2.2.2 Slip Angle - Lateral Force Relation . . . . .	9
2.3 The Magic Formula Tire Model . . . . .	12
<b>3 Road-Holding and Handling Analysis</b>	<b>15</b>
3.1 Road-holding . . . . .	15
3.2 Understeer . . . . .	15
3.2.1 Understeer definition based on yaw velocity . . . . .	16
3.2.2 Understeer based on radius of path of travel . . . . .	16
3.2.3 Understeer based on steering input . . . . .	16
3.2.4 Understeer based on slip angle . . . . .	17
3.3 Handling Diagram . . . . .	18
3.4 Cornering Compliance Method . . . . .	20
3.5 Numerical method for analysing the handling behaviour . . . . .	21
3.6 Tool Development . . . . .	23
<b>4 Validation and Results</b>	<b>27</b>
4.1 Validation of the Model . . . . .	27
4.1.1 Validation using ÅF Test Data . . . . .	27
4.1.2 Validation using AstaZero Test Data . . . . .	29

4.2	Effect of change of centre of gravity location (or weight distribution) on handling of the vehicle . . . . .	30
4.3	Effect of change of roll stiffness distribution on handling of the vehicle	30
4.4	Effect of change of centre of gravity height on handling of the vehicle	31
4.5	Effect of change of roll centre height on handling of the vehicle . . . .	32
<b>5</b>	<b>Discussions</b>	<b>33</b>
<b>6</b>	<b>Conclusion</b>	<b>35</b>
<b>7</b>	<b>Future Work</b>	<b>37</b>
	<b>Bibliography</b>	<b>39</b>
<b>A</b>	<b>Appendix 1</b>	<b>I</b>
A.1	Vehicle Data . . . . .	I
A.2	Tire Data . . . . .	I
A.3	MATLAB Code . . . . .	II
A.4	User Manual . . . . .	VII

# List of Figures

1.1	Purpose . . . . .	2
2.1	General 2 track vehicle model with 4 degrees of freedom . . . . .	3
2.2	Free body diagram of a two track vehicle model . . . . .	4
2.3	Geometric Load Transfer . . . . .	5
2.4	Mechanism of tire lateral force generation . . . . .	7
2.5	Mechanism of tire lateral force generation . . . . .	8
2.6	Contact Patch Deformation . . . . .	9
2.7	Lateral force vs Slip angle . . . . .	10
2.8	Lateral force vs slip angle for several loads . . . . .	11
2.9	Normalized lateral force vs slip angle . . . . .	12
2.10	Curve produced by the Magic Formula . . . . .	13
3.1	Olley's Definition of Understeer . . . . .	16
3.2	Sideslip angle of an understeering vehicle . . . . .	17
3.3	Tireslip angle of an understeering vehicle . . . . .	18
3.4	Single track model in a cornering maneuver . . . . .	18
3.5	Axle Characteristic of a vehicle . . . . .	19
3.6	Axle characteristics and resulting handling curves . . . . .	19
3.7	Tool development . . . . .	23
3.8	Input Sheet . . . . .	24
3.9	Runscript . . . . .	24
3.10	Flowchart of the code . . . . .	25
3.11	Velocity and Acceleration output . . . . .	26
3.12	Handling diagram . . . . .	26
4.1	Test cases obtained from internal report at ÅF . . . . .	27
4.2	Handling Diagram for the 3 setups from ÅF test data . . . . .	28
4.3	Handling Diagram of Theoretical Data from the Model . . . . .	28
4.4	Comparison between ÅF Experimental and Theoretical data . . . . .	29
4.5	Data comparison between test data from AstaZero and the Model . . . . .	29
4.6	Handling Diagram comparison for the Weight Distribution variation . . . . .	30
4.7	Handling Diagram comparison for the Roll Stiffness Distribution variation . . . . .	31
4.8	Handling Diagram for comparing the variation in Centre of Gravity Height . . . . .	31
4.9	Handling Diagram for comparing the Roll Centre Height variation . . . . .	32

A.1	Vehicle Data . . . . .	I
A.2	Tire Data . . . . .	I
A.3	Step1 . . . . .	VII
A.4	Step2 . . . . .	VII
A.5	Step3 . . . . .	VIII
A.6	Step4 . . . . .	VIII

# 1

## Introduction

### 1.1 Background

Ever since the beginning of the automotive era in the 19th century, vehicle dynamics has played an important role in the development of the vehicle industry. Early research in the field of vehicle dynamics concentrated on the vehicle performance under external excitation. In the 1930s, the researchers began to focus on the steering, suspension mechanism, ride comfort and handling dynamics of the vehicle. The handling dynamics deals with the lateral forces generated by the tires, the yaw and the roll dynamics of the vehicle. Vehicle handling is extremely important not just for the safety reasons but also to give a sense of control to the driver which makes driving comfortable and enjoyable.

### 1.2 The Importance of Understeer

In the field of vehicle dynamics, lateral dynamic analysis of the vehicle and the vehicle handling plays an important role. Vehicle handling deals with the response of a vehicle to the inputs provided by the driver. Vehicle handling is thus the response to the acceleration, braking and the steering input. While the response to the propelling and braking inputs are also considered as vehicle handling response, understanding the vehicle's response to the steering input is quite usually the main objective of handling analysis. Two important aspects in the field of vehicle's handling are understeer and road holding. The lateral grip of the vehicle is defined as the capability of the vehicle to maintain grip with the road during cornering and resisting to slide.

Understeer however can be defined in many ways, exploring which is also an objective of this master thesis. In an overview, understeer can be defined as how much the driver needs to change the steering input to maintain a path of constant radius as the vehicle speed is increased. The same can be analysed in another way where the understeer of the vehicle is how much the radius of the vehicle's path will change when the driver has a constant steer angle and increases the speed of the vehicle. Therefore understeer is an important feedback to the driver. The understeer of the vehicle itself is determined by the lateral forces generated at the contact patch of the tires and is a factor of the tire's road holding capability. The lateral utilizable grip is limited by the friction circle. The lateral grip is important because it determines whether or not an obstacle can be avoided when the vehicle is running at a

particular speed.

### 1.3 Purpose

With the refinement in vehicle dynamics analysis and the increase in the demand for development of the vehicles in shorter periods of time, predicting the vehicle behaviour in the design stage is important. While developing the chassis and suspension system for a vehicle, it is thus important to design for the directional controllability of the vehicle. Predicting the impact of various chassis and suspension parameters on road holding and handling of the vehicle during the design stage can be very beneficial for the vehicle development process and a tool to predict the behaviour by a set of chassis and suspension parameters input can be useful for the engineers.



**Figure 1.1:** Purpose

### 1.4 Objective and the scope of the Thesis

The objective of this master thesis is to develop a user friendly tool to analyse the vehicle handling behaviour as a function of suspension and chassis parameters. This tool is expected to help the design engineers make the necessary decisions in the vehicle development phase to obtain the best dynamic performance of the vehicle.

### 1.5 Delimitations

- This thesis does not take into consideration the aerodynamic effects that result in the lateral dynamics of the vehicle
- The body of the vehicle is considered rigid and the effect of body compliance is outside the scope of this project

# Vehicle System Modelling

## 2.1 Vehicle Model and Equations of Motion

Mathematical modelling of the vehicle system is the primary step to analytically describe the vehicle behaviour. A two track model is used to describe the vehicle geometrically and also analyse the dynamics experienced by the vehicle. Equations of motion in the lateral direction and the lateral load transfer during cornering are described in this section to further develop a method to analyse the vehicle handling characteristics.

### 2.1.1 The Two Track Vehicle Model

Figure 2.1 represents a two track vehicle model with 4 degrees of freedom - two translation degrees of freedom in the road plane ( $x$ - $y$ ), and the two rotational degrees of freedom - roll and yaw. The pitch is ignored in this model since it concentrates on the lateral dynamics of the vehicle.

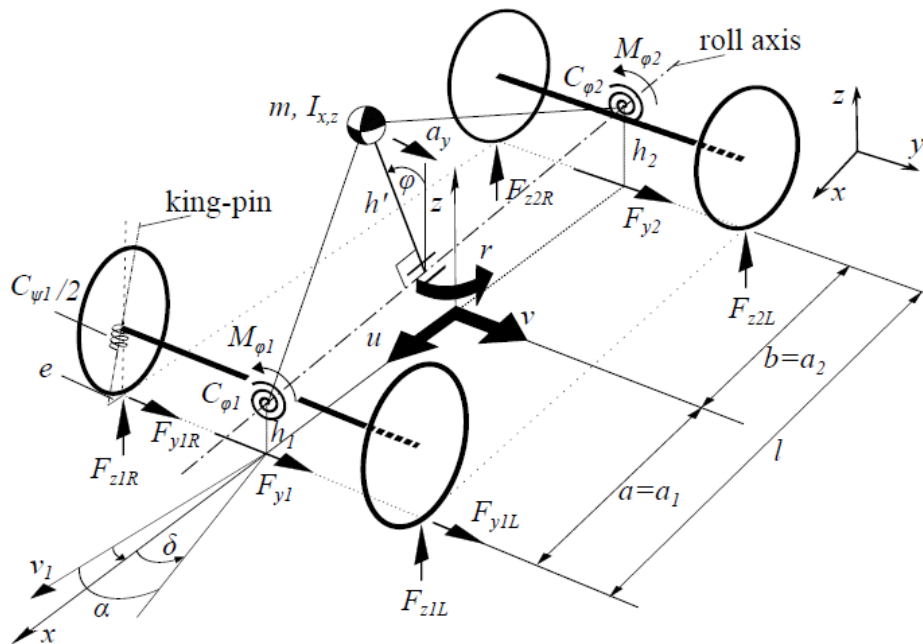


**Figure 2.1:** General 2 track vehicle model with 4 degrees of freedom.

## 2. Vehicle System Modelling

The model includes the vehicle's inertial properties, the effects of suspension and steering system kinematics, compliance such as steer compliance, body roll, lateral load transfer during cornering and also the directional input given by the driver.

The positive  $x$  axis is defined along the length of the vehicle pointing towards the front and lies on the ground plane and on the plane normal to the ground plane and passing through the roll axis. The  $y$  axis points to the left of the vehicle and the  $z$  axis points upward. The  $z$  axis passes through the center of gravity in the absence of a roll angle which is represented by  $\phi$ . The intersection of the three axes define the origin which will be used as a reference point to define other vehicle parameters.

When the vehicle negotiates a corner, the vehicle rolls towards the outside about an imaginary axis called the roll axis. The location and attitude of this virtual axis are defined by the heights of the front and rear roll centers  $h_1$  and  $h_2$ . The roll center locations are governed by the suspension geometry and kinematics.  $c_{\phi 1}$  and  $c_{\phi 2}$  are the front and the rear roll stiffness resulting from the springs and the anti roll bars.

The fore and aft position of the center of gravity in the longitudinal direction is given by  $a_1$  and  $a_2$ , which are the distances from the respective axles. The vertical location is defined by  $h'$ , which is the perpendicular distance of the CoG from the roll axis. The height of the CoG from the ground plane  $h$ .

The body mass and the moment of inertia are defined by  $m$ ,  $I_x$  and  $I_z$ . The mass considers the total mass of the vehicle including the sprung mass and the unsprung mass.

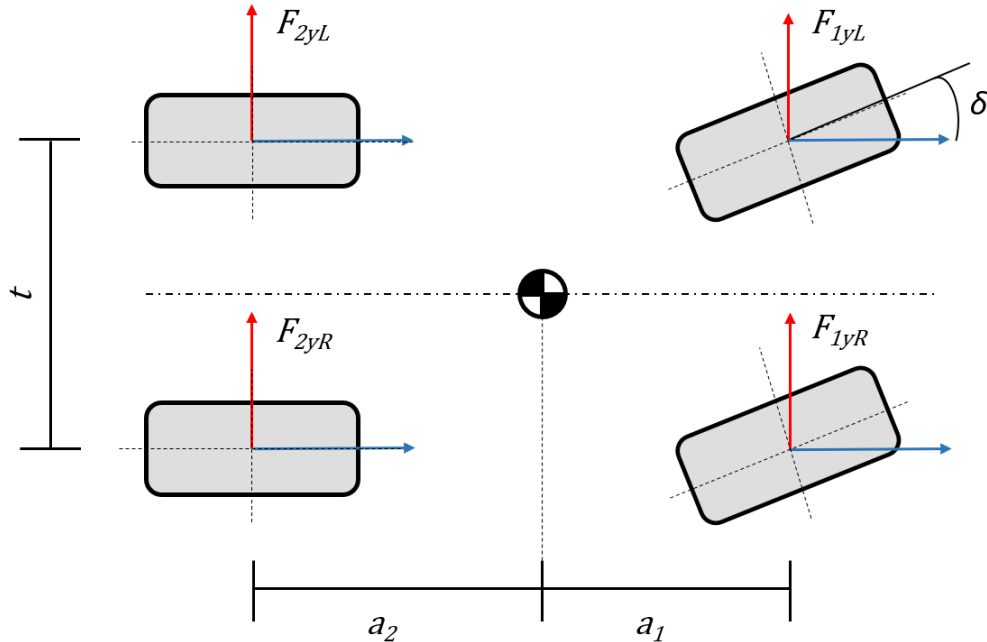


**Figure 2.2:** Free body diagram of a two track vehicle model

Figure 2.2 shows the free body diagram for a two track vehicle model which is maneuvering a left turn. The model assumes the steady state cornering and the



longitudinal dynamics is disregarded. The slip angles are considered to be small and the simplified equations of motion describing the tire lateral forces are shown in the equations below,

$$0 = F_{y1L} + F_{y1R} + F_{y2L} + F_{y2R} - m \cdot a_y \quad (2.1)$$

$$0 = (F_{y2L} + F_{y2R}) \cdot a_2 - (F_{y1L} + F_{y1R}) \cdot a_1 - (I_{zz} \cdot \dot{r}) \quad (2.2)$$

### 2.1.2 Lateral Load Transfer

When a vehicle is cornering in a steady turn, a centrifugal force is developed. The centrifugal force acts towards the outside of the corners and on the vehicle's center of gravity. Since the CoG is located at a distance  $h$  above the ground, a portion of the normal load acting on the tires is transferred from the inside pair of wheels to the outside wheels. Assuming that the vehicle is rigid and contains a single axle, the forces acting on the vehicle can be described as shown in Figure 2.3. The figure describes a rigid vehicle in a steady state right turn.

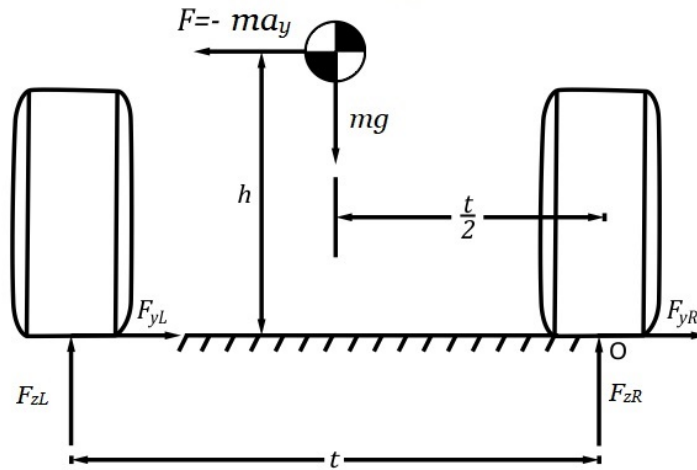


**Figure 2.3:** Geometric Load Transfer

The load transferred to the outer tires can be calculated using the moment equilibrium. Taking the moment about the point O on the right tire,

$$F_{zL} \cdot t = F_z \cdot \frac{t}{2} + m \cdot a_y \cdot h \quad (2.3)$$

The magnitude of the load transferred to the outside wheels is the difference in the instantaneous load on the wheel and the load at zero load transfer. The load transfer can thus be calculated by the equation 2.4

$$\Delta F_z = \frac{mh}{t} \cdot a_y \quad (2.4)$$

The load transfer is thus a function of the center of gravity height  $h$ , the track width  $t$  and the lateral acceleration  $a_y$ . For a vehicle with 2 axles, the overall load transfer is split between the axles in the ratio of the distance of the axles from the center of gravity. The equation for load transfer for a two axle rigid vehicle then becomes,

$$\Delta F_{zi}^{rv} = \frac{mh}{t \cdot l} \cdot (l - a_i) a_y \quad (2.5)$$

where  $i = 1, 2$  represents the front and the rear axles respectively.

Real vehicles show an elastic behaviour and when a considerably high centrifugal force is acting on the vehicle, the phenomenon of body roll occurs. Due to this, the total lateral load transfer is not just a function of track width and the CoG height but is also dependent on roll center heights and the roll stiffness provided by the springs and anti roll bars. The roll dynamics about the roll axis can be expressed as a dynamic equilibrium by the equation 2.6

$$\Sigma M_\phi = (I_x + mh'^2) \ddot{\phi} + c_\phi \dot{\phi} + k_\phi \phi - mh'(a_y + g\phi) = 0 \quad (2.6)$$

where  $c_\phi$  is the total roll stiffness of the vehicle and  $k_\phi$  is the total roll damping. In a steady state cornering situation, the roll rate of the vehicle is zero and hence in the equation (2.6),  $\dot{\phi}$  and  $\ddot{\phi}$  becomes zero. The steady state roll angle  $\phi$  can then be determined by the relation,

$$\phi = \frac{mh'}{(c_{\phi 1} + c_{\phi 2}) - mh'g} a_y \quad (2.7)$$

The front and the rear suspensions are assumed to have fixed roll center height  $h_i$  determined by the layout of the suspension. The height of CoG above the roll axis can be determined as,

$$h' = h - \left( \frac{(h_2 - h_1)}{l} a_1 + h_1 \right) \quad (2.8)$$

The load transfer on the outer wheels including the elastic effects can be determined from the dynamic equilibrium of each axle.

$$\Sigma M_{\phi i} = (F_{zi} - \Delta F_{zi})s - (F_{zi} + \Delta F_{zi})s - c_{\phi i} \cdot \phi - k_{\phi i} \cdot \dot{\phi} - h_i F_{yi} = 0 \quad (2.9)$$

where,  $F_{zi}$  is the load on the wheels at zero load transfer condition and  $\Delta F_{zi}$  is the load transfer. The equation for elastic load transfer can be given as,

$$\Delta F_{zi} = \frac{1}{2s_i} (c_{\phi i} \phi + k_{\phi i} \dot{\phi} + h_i F_{yi}) \quad (2.10)$$

At steady state cornering condition, we have  $\dot{\phi} = 0$ . By combining the equations 2.7 and 2.10, the lateral load transfer at steady state cornering can be determined as

$$\Delta F_{zi}^{ss} = \frac{1}{2s_i} \left( \frac{c_{\phi i}}{c_{\phi 1} + c_{\phi 2} - mh'g} h' + \frac{l - a_i}{l} h_i \right) m a_y \quad (2.11)$$

## 2.2 The Tire

The tire is the only contact between the road and the vehicle and naturally, the tire properties are of high importance in the vehicle dynamics. The pneumatic tires which are essentially the only type of tires found on the motor vehicles today, provide the force that primes the vehicle into motion. Slip angle is an important parameter in the force generation capacity of the tires and is a major part of the description in this section.

### 2.2.1 Slip Angle

The force generated by the vehicle for propulsion and braking comes from the tires. This force is generated at the tire contact patch and is used to accelerate or decelerate the vehicle in the desired direction. The lateral force produced at the tires is a result of the deformation of the rubber at the contact patch. The working of a pneumatic rubber compound tire can be thought of as a spring which stores energy when subjected to a deformation and releases the stored energy when the deformation does not hold any longer. Two experiments described and explained by William and Douglas Milliken in *Race Car Vehicle Dynamics* [3] is a great aid to understand the slip angles and it's profound importance in vehicle dynamics.

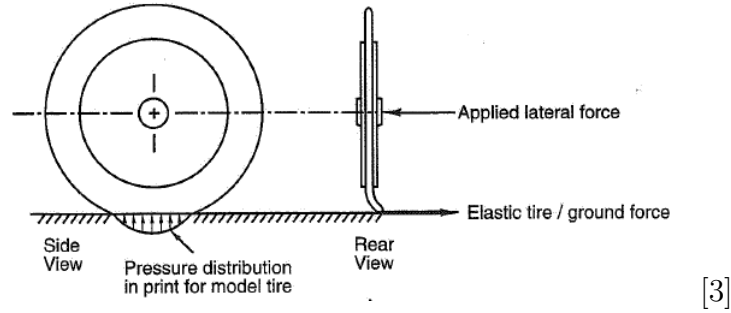


**Figure 2.4:** Mechanism of tire lateral force generation

Figure 2.4 shows a stationary rubber tire placed on the ground. When a lateral force is applied at the rotational axis of the tire, a lateral deflection of the rubber arises in the vicinity of the contact patch. As the wheel starts to roll forward, as shown in Figure 2.5, it will be observed that the direction of heading of the wheel is at an angle  $\alpha$  to the direction of pointing of the wheel. The rubber compound of the tire essentially adheres to the ground at the contact patch while the rest of the tire moves outwards laterally because of the applied lateral force. As the tire rotates, the

part of the tire coming in contact with the ground is offset with the existing contact patch location and this causes a lateral deflection in the contact patch. This lateral deflection relative to the wheel plane continues to grow until the trailing edge of the contact patch. Here, the local vertical force decreases and the frictional force will no longer be sufficient to maintain the developed lateral distortion. At this point, the tire tread rapidly moves back to the wheel center plane releasing the stored energy which is the lateral force.

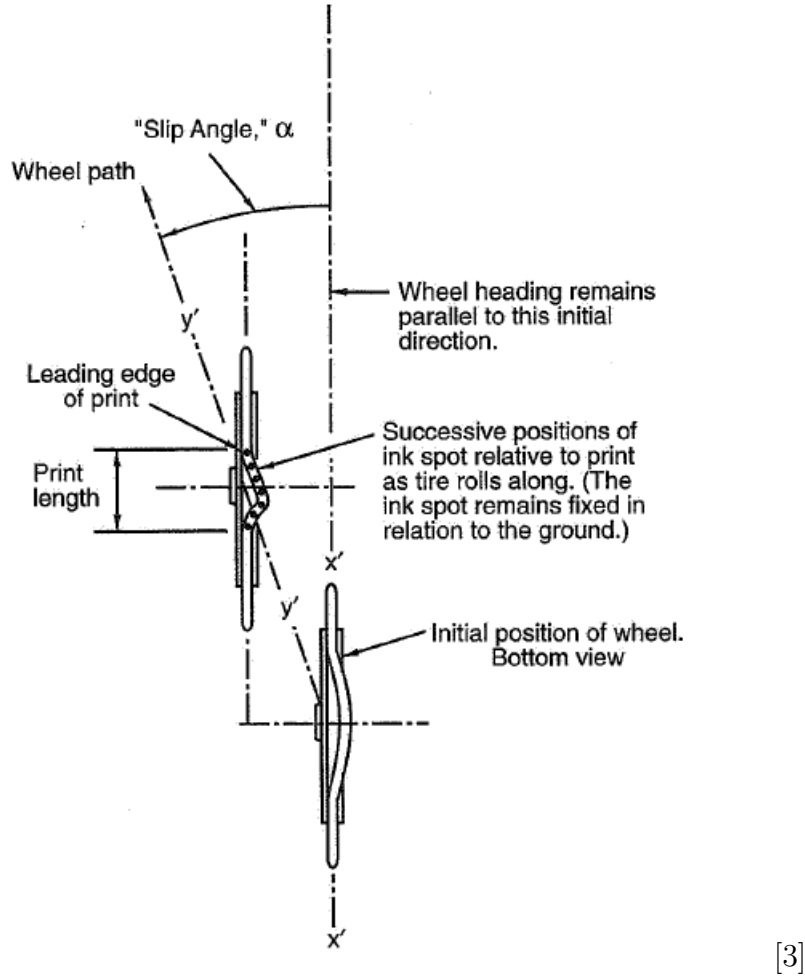


**Figure 2.5:** Mechanism of tire lateral force generation

This resulting angle formed between the heading direction and the pointing direction of the tire is called the slip angle. Although the wheel is not actually slipping in the contact patch in reality, 'slip' angle is somewhat a *misnomer*.<sup>[3]</sup>

The slip angle can be mathematically determined by the ratio of the lateral velocity and the longitudinal velocity of the tire.

$$s_y = \tan(\alpha) = -\frac{v_y}{v_x} \quad (2.12)$$

where,  $s_y$  is the lateral slip,  $\alpha$  is the slip angle,  $v_x$  is the tire longitudinal velocity and  $v_y$  is the tire lateral velocity. The sign convention is chosen such that the force

generation is positive for positive slip angles. At lower slip angles,  $\tan\alpha \approx \alpha$  and hence  $s_y \approx \alpha$ .

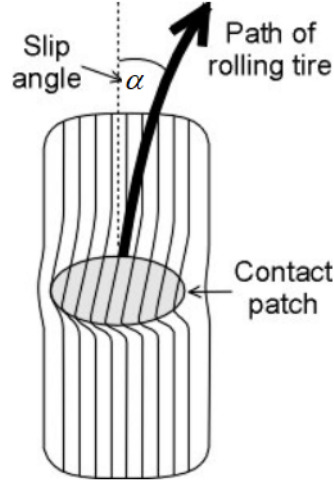


**Figure 2.6:** Contact Patch Deformation

The lateral force and the slip angles may be thought of as the result of one another depending on the type of application. In the example above, the applied external lateral force resulted in a slip angle. However in an automobile, when the front wheels are steered a slip angle is created due to the steering geometry, which gives rise to a lateral force required to move the vehicle in the lateral direction.

### 2.2.2 Slip Angle - Lateral Force Relation

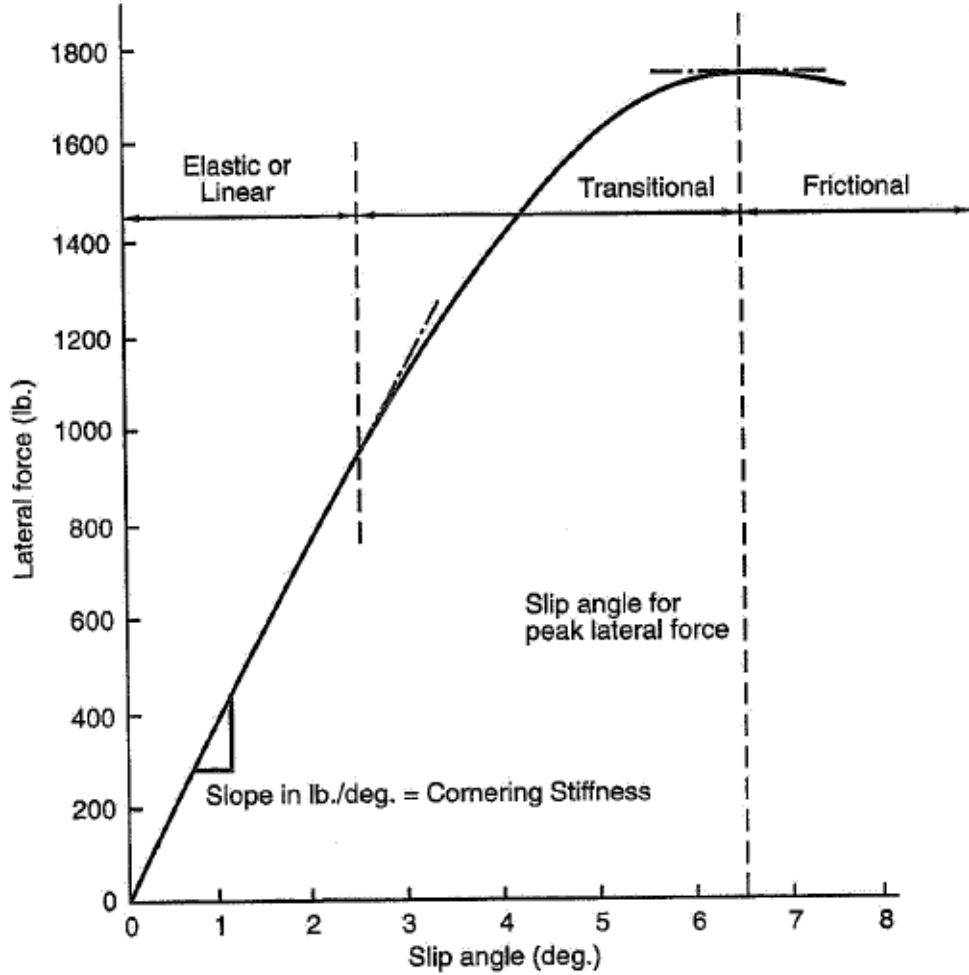
The lateral force thus generated at the tires can be represented as a function of slip angle for the practical automotive applications. Figure 2.7 shows the empirical data for the lateral force - slip angle relation.

It can be observed from the figure that at lower slip angles, the lateral force generated by the tire is approximately a linear function of the slip angles and becomes non linear at higher slip angles. The lateral force reaches a peak value limited by the road friction and then falls down with the further increase in the slip angles. In the automotive applications of passenger cars, the tires normally operate within the linear or elastic region. The non linear region of the tires can be reached when the vehicle is subjected to a considerably high lateral acceleration. A good approximation for the determination of the lateral force for small slip angles can be given by a linear relation as given in the equation 2.13

$$F_y = -C_\alpha \cdot \alpha \quad (2.13)$$

The term  $C_\alpha$  is called as the lateral slip stiffness or cornering stiffness. The cornering stiffness of a tire is defined as the derivative of the lateral force with respect to slip angle at  $\alpha = 0$ . [9]

$$C_\alpha = -\left(\frac{\partial F_y}{\partial \alpha}\right)\bigg|_{\alpha=0} \quad (2.14)$$



[3]

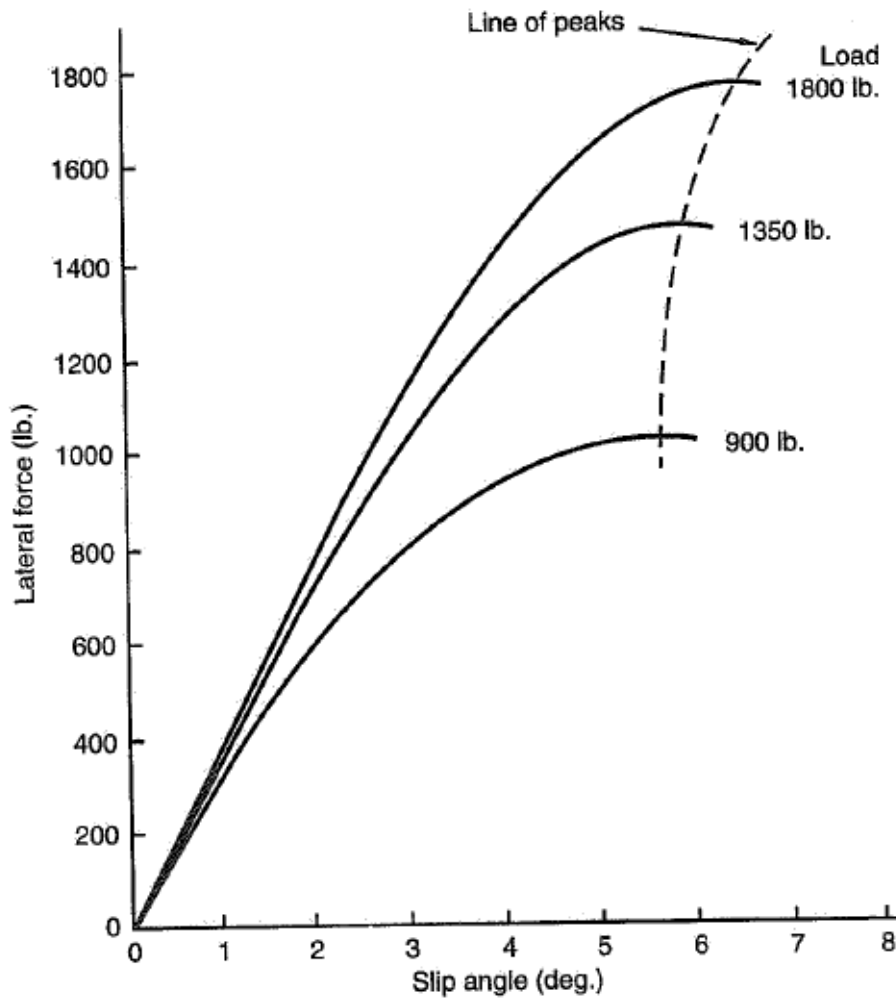
**Figure 2.7:** Lateral force vs Slip angle

The lateral force is a function of various parameters such as slip angle  $\alpha$ , brake slip  $\kappa$ , wheel camber  $\gamma$  and the normal force  $F_z$ .

$$F_y = F_y(\kappa, \alpha, \gamma, F_z) \quad (2.15)$$

Several other factors like tire pressure, tire temperature, tread pattern, tire wear etc., contribute to the tire characteristics, but this exhaustive list will not be explored within the scope of this study. The effects of camber angle and the combined slip condition are disregarded and the lateral force characteristics of the tire is considered at pure slip conditions only; meaning that the brake slip is zero.

The lateral force generation capability of the tires is dependent on the normal load. An interesting relationship with the lateral force and the normal force can be observed in the pneumatic rubber tires. The general behaviour of the tire's cornering performance as a function of vertical load is presented in Figure 2.8.

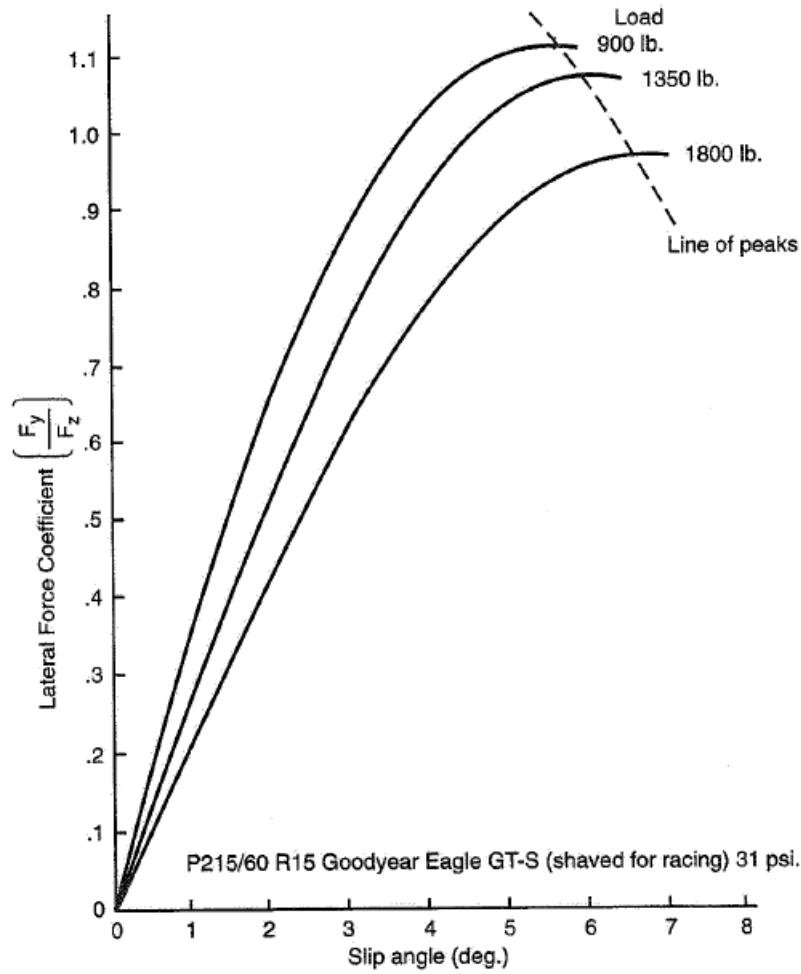


[3]

**Figure 2.8:** Lateral force vs slip angle for several loads

It can be observed that, for a given slip angle, a tire can generate higher lateral force for a higher normal load. But interestingly, when the lateral force generation capability per normal load is considered, an inverse relation is observed. That is, for normalized lateral force with the vertical load, the capacity of the tires to generate cornering force decreases with the increase in the normal load. This normalized lateral force  $\frac{F_y}{F_z}$  is called the lateral force coefficient and from Figure 2.9 it can be seen that the peak lateral coefficient is higher for lighter loads and falls off as the load increases [3]. This effect is called the tire load sensitivity.

A relation can be drawn to the load transfer here. When the load transfers to the outer tires during cornering, the increase in the lateral force by the outer tires is less in than the decrease in the lateral force of the inner tires. This reduces the effective force generating capability of an axle under the influence of the load transfer. Therefore an axle experiencing lateral load transfer can not produce the same amount of lateral force that it is capable of producing in the absence of load transfer.



[3]

**Figure 2.9:** Normalized lateral force vs slip angle

### 2.3 The Magic Formula Tire Model

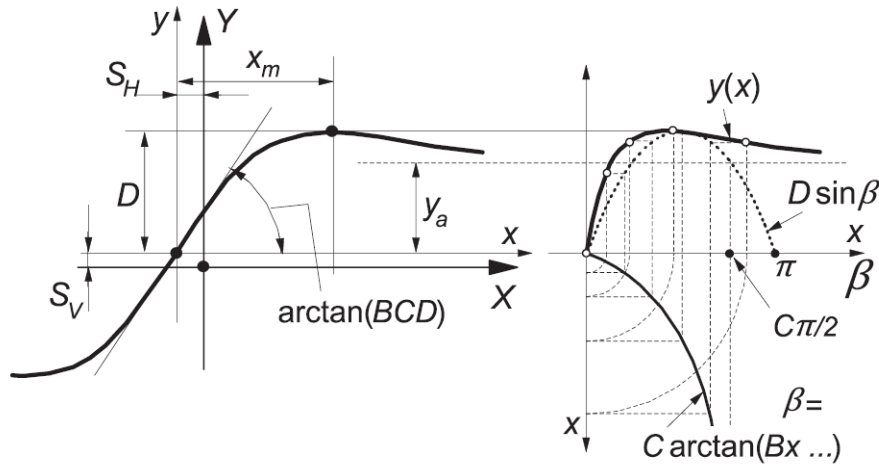
By describing the tire properties discussed in the previous chapter mathematically, an engineer can analyse, simulate and predict the vehicle behaviour. Tire modelling is an important aspect of vehicle dynamics. The mathematical tire model that expresses the non linear relation between the slip angles and the lateral force thus becomes essential. Over the years, a considerable number of tire models for the description of force and moment generating properties have been described. The physical models or the theoretical tire models are based on the physical nature of the tire whereas empirical models depend on the experimental data. The Magic Formula tire model is a widely used semi-empirical tire model that is used to calculate the steady state tire characteristics. This tire model is formed based on a formula popularly known as the Magic Formula [4]. Several versions of this formula have been developed since the mid 18th century and the formula is capable of producing tire force and moment characteristics for pure slip conditions.



The general form of the Magic formula tire model is given by the relation,

$$y = D \cdot \sin[C \cdot \tan^{-1}\{Bx - E(Bx - \tan^{-1}Bx)\}] \quad (2.16)$$

where,  $y$  is the output variable which can take the form of the longitudinal force  $F_x$ , lateral force  $F_y$  or even possibly the aligning moment  $M_z$ .  $x$  is the corresponding input variable, which will either be longitudinal slip  $\kappa$  or slip angle  $\tan\alpha$ .  $B$ ,  $C$ ,  $D$  and  $E$  are the magic formula parameters where  $B$  is the stiffness factor,  $C$  is the shape factor,  $D$  is the peak value and  $E$  is the curvature factor.[5]



[5]

**Figure 2.10:** Curve produced by the Magic Formula

The Magic Formula typically produces a curve that passes through the origin  $x = y = 0$ , reaches a maximum, and subsequently tends to a horizontal asymptote. While the equation 2.13 provides the lateral force generated at lower slip angles, the Magic formula can determine the lateral force generated even in the non linear operating area of the tire.

Figure 2.10 illustrates the meaning of the parameters used in the Magic Formula. The peak value  $D$  represents the maximum lateral force that can be developed which is limited by the friction coefficient  $\mu$ . The product of the parameters  $B$ ,  $C$  and  $D$  corresponds to the slope at origin and can be considered equivalent to the cornering stiffness of the tire  $C_\alpha$  at zero camber angles. The shape factor  $C$  controls the limits of the range of sine function and thereby determines the shape of the curve. The stiffness factor  $B$  is left to determine the slope of the curve at origin. The curvature factor  $E$  controls the curvature at the peak and also the horizontal location of the peak. Parameters  $S_H$  and  $S_V$  simply shift the curve in horizontal and vertical axes so that the curve passes through the origin, which might not be the case for some measurement data due to some errors. Factors  $B$ ,  $D$  and  $E$  are functions of the vertical load and a full set of equations to determine these parameters are presented here.

**Magic formula parameters for Lateral force**

$$F_y = D \cdot \sin[C \cdot \tan^{-1}\{B\alpha - E(B\alpha - \tan^{-1}B\alpha)\}] \quad (2.17)$$

$$C = p_{Cy} \cdot \lambda_{Cy} \quad (2.18)$$

$$D = \mu_y \cdot F_z \cdot \xi_2 \quad (2.19)$$

$$\mu_y = (p_{Dy1} + p_{Dy2} df_z)(1 + p_{py3} dp_i + p_{py4} dp_i^2) \quad (2.20)$$

$$E = (p_{Ey1} + p_{Ey2} df_z) \quad (2.21)$$

$$K_{y\alpha} = p_{Ky1} F_{z0}(1 + p_{py1} dp_i) \cdot \sin \left[ p_{ky4} \tan^{-1} \left\{ \frac{F_z/F'_{zo}}{p_{Ky2} + (1 + p_{py2} dp_i)} \right\} \right] \cdot \xi_3 \lambda_{Ky\alpha} \quad (2.22)$$

$$B_y = K_{y\alpha}/(C_y D_y) \quad (2.23)$$

$$df_z = \frac{F_z}{F_{z0}} \quad (2.24)$$

It can be observed here that the factors  $D$ ,  $E$  and  $B$  are the functions of normal load  $F_z$  and during cornering with lateral load transfer, the normal load on all the tires will be different. Which would mean that the lateral force generated at each tire will be different. The magic formula needs to be applied individually to all the tires to calculate the lateral force based on the normal load. From the equation 2.11, the normal load on all the tires can be calculated using the following relation.

$$F_{z1i} = \frac{F_{z10}}{2} - \Delta F_{z1}^{ss} \quad (2.25)$$

$$F_{z1o} = \frac{F_{z10}}{2} + \Delta F_{z1}^{ss} \quad (2.26)$$

$$F_{z2i} = \frac{F_{z20}}{2} - \Delta F_{z2}^{ss} \quad (2.27)$$

$$F_{z2o} = \frac{F_{z20}}{2} + \Delta F_{z2}^{ss} \quad (2.28)$$

The magic tire formula for each tire will then become,

$$F_{y,ij} = D_{ij} \cdot \sin[C_{ij} \cdot \tan^{-1}\{B_{ij}\alpha - E_{ij}(B_{ij}\alpha - \tan^{-1}B_{ij}\alpha)\}] \quad (2.29)$$

where  $i = 1, 2$  and  $j = i, o$  represent the front and rear axles and inner and outer tires.

The typical values of the model parameters for the Magic Formula tire model for common road conditions are given in the Table 2.1

**Table 2.1:** Typical parameter values of Magic Formula

Surface	B	C	D	E
Dry Tarmac	10	1.9	1	0.97
Wet Tarmac	12	2.3	0.82	1
Snow	5	2	0.3	1
Ice	4	2	0.1	1

# 3

## Road-Holding and Handling Analysis

### 3.1 Road-holding

As discussed previously in the section 2.2.1, the tire tread in the contact patch adheres to the road surface and during cornering, the deformation in the contact patch generates the lateral force required to counteract the centrifugal force. Road holding is the capability of the tires to retain this grip with the road. At significantly higher lateral accelerations, the tire loses its capability to hold to the road surface and starts to slide. The maximum point at which the tire holds or adheres to the road is called the *Limit of Adhesion*.

A vehicle can only be predictable and controllable until the tires retain grip with the road. As discussed in the section 2.2.1 the slip angle is generated in the tire because of the deformation of the contact patch. When the deformation becomes large, the tire can no longer adhere to the road and the tire starts to lose grip. If the grip is lost in the front tires, the tires start to slide outside of the curve and the steering input will stimulate very little to no response from the vehicle. However, if the rear tires lose the grip, the sliding of the rear tires pushes the vehicle into instability.

It hence becomes important to evaluate the vehicle characteristics so that the vehicle behaviour can be estimated theoretically and observed objectively. Understanding and quantifying the understeering nature of the vehicle can be an effective way of analysing the vehicle handling and is presented in the subsequent sections.

### 3.2 Understeer

Understeer and oversteer are the vehicle's characteristic responses that can be used to determine the handling behaviour of the vehicle. These phenomena can be defined in several ways depending upon the type of input. The different definitions lead to the same understanding of understeer but uses different approaches to describe and quantify understeer. The definitions are discussed in the subsequent sections and the chosen approach to this thesis is presented.

#### 3.2.1 Understeer definition based on yaw velocity

The phenomenon of understeer can be defined based on the change in yaw velocity of the vehicle with the change in lateral acceleration. When an external force is applied to the center of gravity of a freely moving vehicle with zero steer angle, an understeering vehicle would develop a yaw velocity in a direction away from the input force as shown in Figure 3.1. An oversteering vehicle would curve towards the direction of the force and a neutral steer vehicle would develop no yaw velocity, but will move at an angle to the initial path.

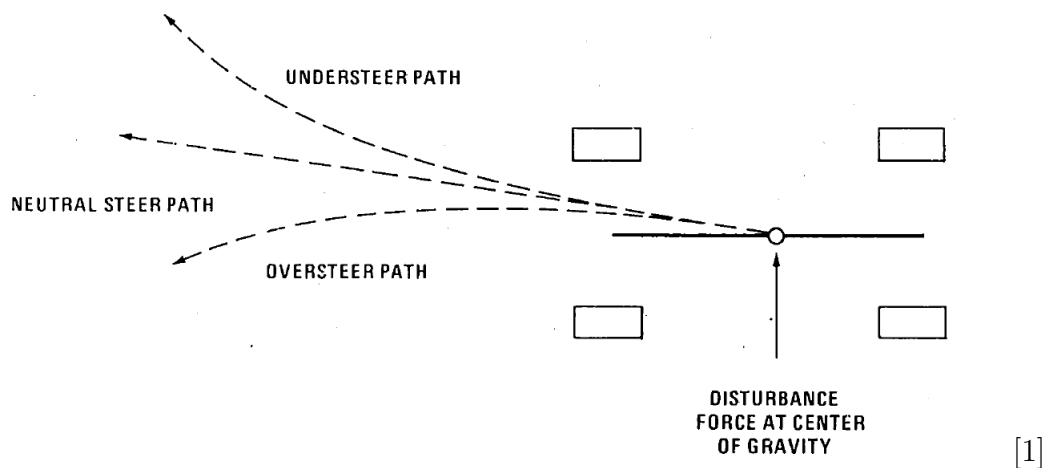


**Figure 3.1:** Olley's Definition of Understeer

The lateral acceleration of the vehicle is changed as a result of an external force in this case. Crosswinds and aerodynamic effects are some examples of such an external influence on the vehicle's lateral acceleration. The study of vehicle handling is more appropriate in a cornering situation rather than the response to external stimulation. The understanding of understeer in a cornering situation leads to another approach to define understeer based on the change in the radius path of travel.

#### 3.2.2 Understeer based on radius of path of travel

For a vehicle cornering with a constant steer angle, understeer and oversteer can be defined as the resultant change in the radius of the path of travel with changing lateral acceleration. An increase in the path radius with increasing lateral acceleration indicates that the vehicle is understeering and conversely, a decrease in the path radius with increasing lateral acceleration suggests that the vehicle is oversteering. A neutral steer vehicle will undergo no change in the radius of path with a change in lateral acceleration.

#### 3.2.3 Understeer based on steering input

When the front wheels of a vehicle are steered, the vehicle develops a yawing moment due to the geometry. The lateral force produced by the tires during cornering

generates a secondary yawing moment. If the secondary yawing moment produced by the steering input resists the primary moment developed due to the steering geometry, then the vehicle is said to be understeered.[2] If the secondary yawing moment assists the primary yawing moment, the vehicle is said to be oversteered. A vehicle that develops no secondary yawing moment is neutral steered. In other words, to be able to travel along the circular path of the fixed radius with increase in lateral acceleration, steering angle must be increased in an understeering vehicle and decreased in an oversteering vehicle. This is the same concept of the definition based on the change in radius but represented in terms of required steering angle.

### 3.2.4 Understeer based on slip angle

One of the most commonly used definition of understeer is based on the slip angle difference in the front and the rear axle. According to this definition, the vehicle is understeered if the slip angle of the front tires are greater than the slip angle of the rear tires and oversteered if the slip angle of the rear tires is greater than the slip angle of the front tires. However, this definitions holds only when the tires in the front and the rear axles are the same. As discussed in the section 3.1, when the slip angle becomes large, the tires can lose grip and change the vehicle's yaw or the radius of path of travel.

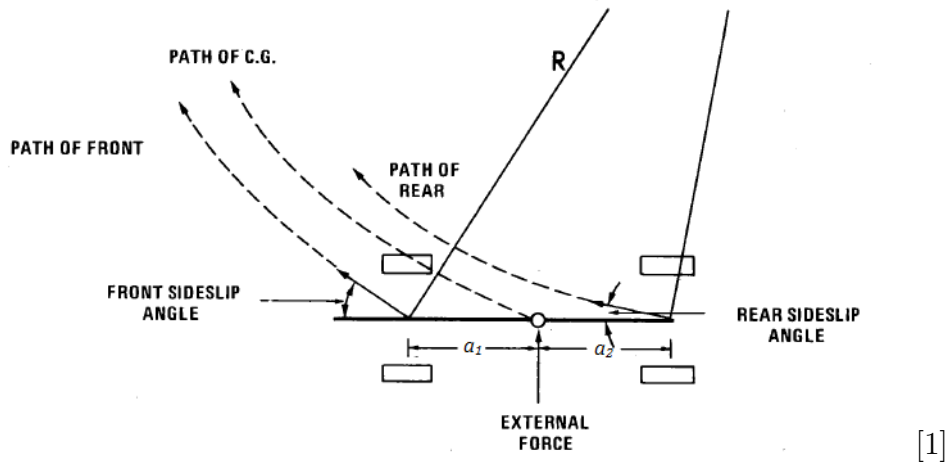


**Figure 3.2:** Sideslip angle of an understeering vehicle

Figure 3.2 shows the sideslip angles of the front and the rear axles. Sideslip angle refers to the relative motion of the vehicle body and the road. But for the calculation of understeer, it is reasonable to consider the tire slip angles. Figure 3.3 shows the front and the rear slip angles of the tires.

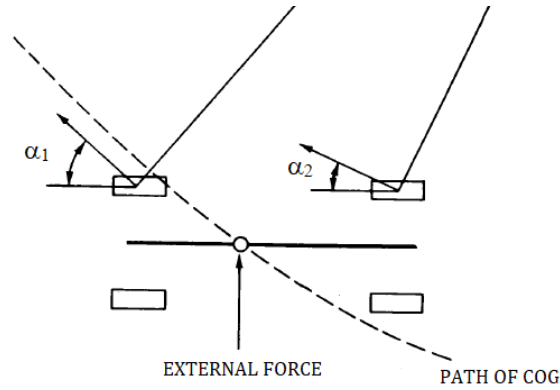
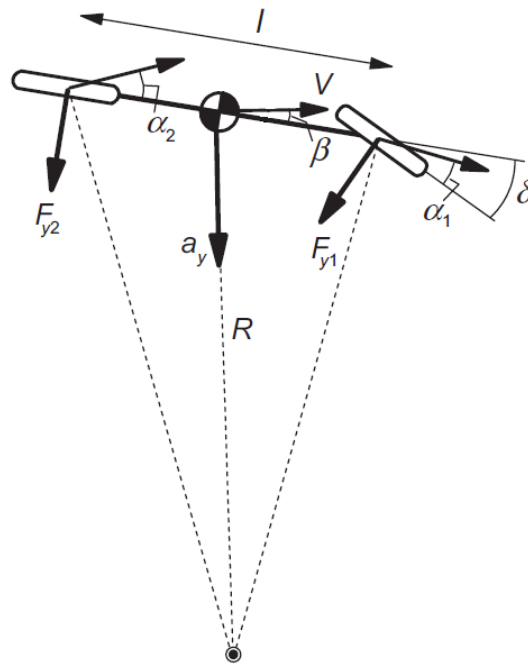


**Figure 3.3:** Tireslip angle of an understeering vehicle

The definition of understeer based on slip angles is selected for the detailed study of this thesis since the difference in the front and rear slip angles can be used to generate a handling diagram which can be further used to relate to the other definitions of understeer.

### 3.3 Handling Diagram

The handling diagram is a method used to assess the vehicle characteristics and is similar to the experimental results obtained from tests such as steady state cornering. The handling diagram is an useful tool to correlate the slip angles in the front and the rear axles with the lateral acceleration acting on the vehicle. Figure 3.4 depicts the single track vehicle model in a steady-state cornering maneuver.



[5]

**Figure 3.4:** Single track model in a cornering maneuver

The normalized lateral force of the axles is given by the following relation.

$$\frac{F_{y1}}{F_{z1}} = \frac{F_{y2}}{F_{z2}} = \frac{a_y}{g} \quad (3.1)$$

The ratio of the side force and vertical load as shown in the equation 3.1 plotted as the function of the slip angle is termed as the normalized tire or axle characteristics. These characteristics subtracted horizontally from each other produces the handling curve or the handling diagram. Considering the equality from 3.1, the ordinate of the graph can be replaced by  $a_y/g$ . Figure 3.6 shows a set of four possible combinations of axle characteristics together with the resulting handling curves.

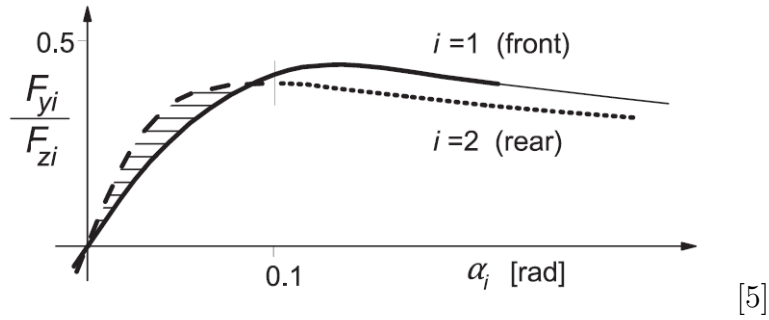


**Figure 3.5:** Axle Characteristic of a vehicle

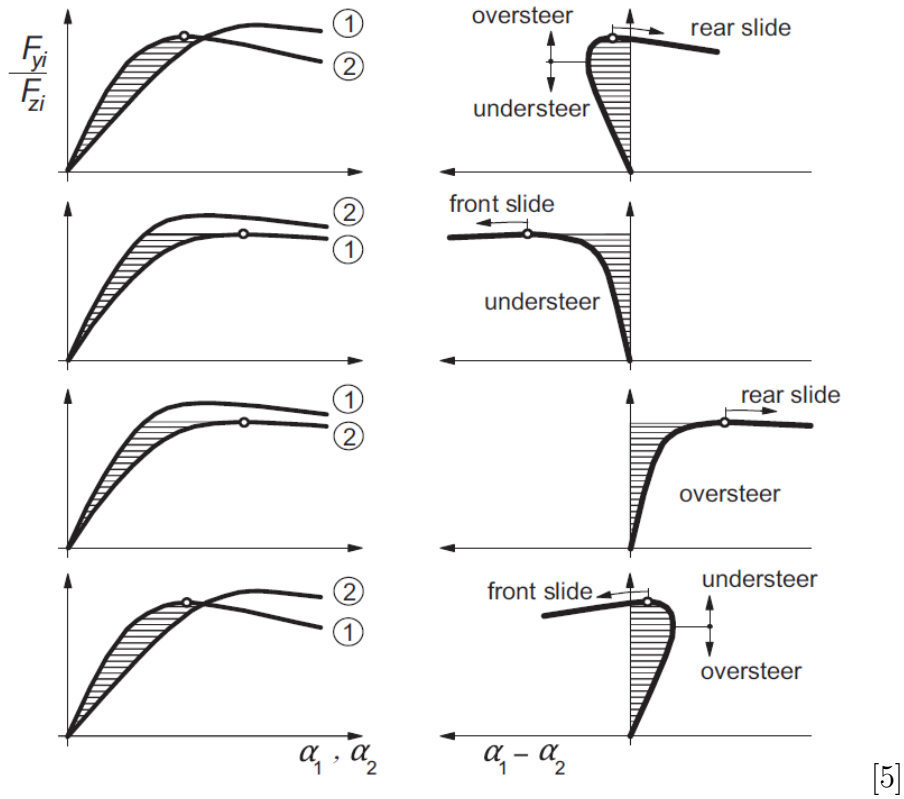


**Figure 3.6:** Axle characteristics and resulting handling curves

### 3.4 Cornering Compliance Method

For relatively small lateral accelerations, linear approximation of the cornering characteristics hold valid which consider just the slope at zero slip condition. The side force generated by the tires follows a linear relationship with the slip angles as specified in the equation 2.13 in the page 9. Figure 3.4 is a single track representation of a vehicle of mass  $m$  in a steady state cornering situation. The forward velocity of the vehicle is  $v_x$  and the path radius is  $R$ . The geometry of the turn can be described by the relation below.

$$\frac{l}{R} = \delta - (\alpha_1 - \alpha_2) \quad (3.2)$$

The lateral force generated at the tires are distributed among the axles in the proportion of the static normal force acting on the axle.

$$F_y = \frac{mv_x^2}{R} = ma_y \quad (3.3)$$

$$F_{y1} = \frac{l - a_1}{l} F_y = \frac{a_2}{l} \cdot ma_y \quad (3.4)$$

$$F_{y2} = \frac{l - a_2}{l} F_y = \frac{a_1}{l} \cdot ma_y \quad (3.5)$$

The values of the slip angles in the front and the rear can be determined by the following equations where,  $C_{\alpha,eff1}$  and  $C_{\alpha,eff2}$  are respectively the front and rear effective axle cornering stiffness.

$$\alpha_1 = \frac{F_{y1}}{C_{\alpha,eff1}} \quad (3.6)$$

$$\alpha_2 = \frac{F_{y2}}{C_{\alpha,eff2}} \quad (3.7)$$

For the chosen definition for understeer, the difference in the front and the rear slip angle needs to be determined. The difference in the slip angles can be expressed as,

$$\alpha_1 - \alpha_2 = \left[ \frac{F_{y1}}{C_{\alpha,eff,1}} - \frac{F_{y2}}{C_{\alpha,eff,2}} \right] \quad (3.8)$$

$$\alpha_1 - \alpha_2 = \left[ \frac{ma_y \cdot a_2}{l \cdot C_{\alpha,eff,1}} - \frac{ma_y \cdot a_1}{l \cdot C_{\alpha,eff,2}} \right] \quad (3.9)$$

By normalizing the equation 3.8 with the vertical load, we can obtain the cornering characteristics as a function of the acceleration in  $g$  terms.

$$\alpha_1 - \alpha_2 = \left[ \frac{mg \cdot a_2}{l} \frac{1}{C_{\alpha,eff,1}} - \frac{mg \cdot a_1}{l} \frac{1}{C_{\alpha,eff,2}} \right] \frac{ma_y}{mg} \quad (3.10)$$



$$\alpha_1 - \alpha_2 = \left[ \frac{F_{z1}}{C_{\text{eff},1}} - \frac{F_{z2}}{C_{\text{eff},2}} \right] \frac{a_y}{g} \quad (3.11)$$

$$\alpha_1 - \alpha_2 = \eta \frac{a_y}{g} \quad (3.12)$$

where,  $\eta$  is the understeer gradient. For lower levels of lateral acceleration, this method can produce a good handling diagram to analyse the axle characteristics.

### 3.5 Numerical method for analysing the handling behaviour

While cornering at higher velocities, the vehicle experiences higher lateral accelerations and the linear approximations mentioned in the above methodology becomes invalid. The value of cornering stiffness at the zero slip conditions can not be used to accurately understand the handling behaviour at higher lateral accelerations. Linearization of tire curve can be made at the point of operation to determine the equivalent cornering stiffness but a numerical method of solving the equations of motion is presented here.

The non linear equations describing the slip angles, the force balance in the axles, the individual tire lateral forces and the steering to slip angle relation are solved simultaneously to obtain the value of the front and the rear slip angles. This method can accurately determine the slip angles until the limit of adhesion and the understeer behaviour of the vehicle can be analysed by plotting the data into a handling diagram.

The slip angles in the inner and the outer tires are significantly different at higher velocities. The equations for slip angles at each tire are given by

$$\alpha_{1,in} = \delta_{rw} - \left( \frac{v_y + a_1 r}{v_x - s_1 r} \right) \quad (3.13)$$

$$\alpha_{1,out} = \delta_{rw} - \left( \frac{v_y + a_1 r}{v_x + s_1 r} \right) \quad (3.14)$$

$$\alpha_{2,in} = - \left( \frac{v_y - a_2 r}{v_x - s_2 r} \right) \quad (3.15)$$

$$\alpha_{2,out} = - \left( \frac{v_y - a_2 r}{v_x + s_1 r} \right) \quad (3.16)$$

where,  $\delta_{rw}$  is the road wheel angle,  $r$  is the yaw rate of the vehicle and  $s_1$  and  $s_2$  are the front and rear track width.

With different slip angles for the individual tires, the lateral force generated at each tire can be determined using the Magic Formula tire model.

$$F_{y1,in} = D \cdot \sin[C \cdot \tan^{-1}\{B\alpha_{1,in} - E(B\alpha_{1,in} - \tan^{-1}B\alpha_{1,in})\}] \quad (3.17)$$

$$F_{y1,out} = D \cdot \sin[C \cdot \tan^{-1}\{B\alpha_{1,out} - E(B\alpha_{1,out} - \tan^{-1}B\alpha_{1,out})\}] \quad (3.18)$$

$$F_{y2,in} = D \cdot \sin[C \cdot \tan^{-1}\{B\alpha_{2,in} - E(B\alpha_{2,in} - \tan^{-1}B\alpha_{2,in})\}] \quad (3.19)$$

$$F_{y2,out} = D \cdot \sin[C \cdot \tan^{-1}\{B\alpha_{2,out} - E(B\alpha_{2,out} - \tan^{-1}B\alpha_{2,out})\}] \quad (3.20)$$

The parameters D, B and E are functions of vertical load as mentioned in the section 2.3 and will vary with lateral load transfer. The total lateral force acting on the vehicle is the sum of lateral forces generated by all the tires.

$$ma_y = F_{y1,in} + F_{y1,out} + F_{y2,in} + F_{y2,out} \quad (3.21)$$

The axle lateral force is the sum of the lateral forces developed by the two tires on that axle.

$$F_{y1} = F_{y1,in} + F_{y1,out} \quad (3.22)$$

$$F_{y2} = F_{y2,in} + F_{y2,out} \quad (3.23)$$

The force balance equations for the two axles can be determined by the relation

$$F_{y1} = ma_y \left( \frac{l - a_1}{l} \right) \quad (3.24)$$

$$F_{y2} = ma_y \left( \frac{l - a_2}{l} \right) \quad (3.25)$$

The average slip angle of the left and the right tires is considered as the effective slip angle of the axle. The front and the rear axle slip angles thus are represented by the following equations.

$$\alpha_1 = (\alpha_{1,in} + \alpha_{1,out})/2 \quad (3.26)$$

$$\alpha_2 = (\alpha_{2,in} + \alpha_{2,out})/2 \quad (3.27)$$

It was seen previously in the vehicle geometry that the slip angles and the road wheel angle are given by the relation

$$\delta_{rw} = \frac{l}{R} + (\alpha_1 - \alpha_2) \quad (3.28)$$

The road wheel angle in an ideal and theoretical situation would just be the steering wheel angle divided by the steering ratio. Practically, a compliance in steering arises due to various reasons such as side force and aligning moment. The magnitude of the

compliance is dependent on the caster trail, pneumatic trail and also the steering column torsional stiffness. The moment equilibrium about the steer axis can be mathematically represented as,

$$F_{y1}(e + p) = n_{st}k_{\delta}(\delta_{sw} - \delta_{rw}n_{st}) \quad (3.29)$$

where  $e$  is caster trail,  $p$  is pneumatic trail,  $n_{st}$  is the steering ratio,  $\delta_{sw}$  is the steering wheel angle and  $k_{\delta}$  is the steering column torsional stiffness.

These set of non linear equations can be solved simultaneously using a numerical approach with the help of software intervention. The *fsolve* command in Matlab is used to solve the set of equations which provide the solutions for slip angles of all the tires individually. Since the linear approximation is not made, this solution will be valid for all the levels of lateral acceleration until the limit of adhesion. The calculation of the understeer gradient now reduces to a simple arithmetic subtraction of the slip angles at front and rear. The handling diagram can then be plotted to understand the handling characteristics of the vehicle with progressive lateral acceleration.

### 3.6 Tool Development

It is important for the vehicle design engineers to be able to develop the suspension system that influences a predictable directional control. Having a tool that can simulate the vehicle handling behaviour for a given set of suspension setup can be very helpful for the designers to make important decisions and trade offs in the early stage of vehicle development. This thesis aims at developing such a tool that can provide information on the dependence of understeer on suspension parameters, while being simple to use and providing reliable results. The tool is designed to be simple to use, and provide quick results. The input interface is an excel file which is fed into a m-file in Matlab. By running the script, the code initiates a function file which runs in the background. This way, the source code is protected from any unintentional changes that might happen with the user error. The tool provides the information of maximum linear velocity achievable in a given radius of path curvature, the corresponding maximum lateral acceleration and the handling diagram.

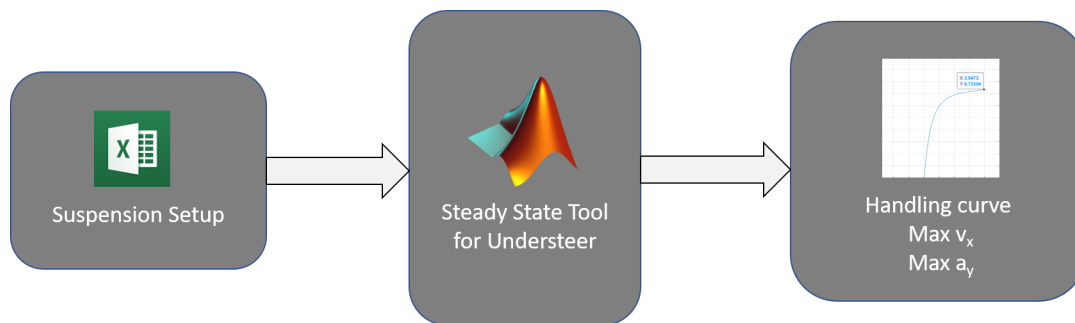


**Figure 3.7:** Tool development

### 3. Road-Holding and Handling Analysis

The input file contains various suspension parameters such as mass distribution, total roll stiffness, roll stiffness distribution, roll center height, center of gravity height etc., and also the tire parameters. The tool uses the magic formula tire model to calculate the lateral forces. The input file is shown in Figure 3.8

Suspension Parametes Impact on Understeer - Input Sheet

Configuration name:Config1

Date:25-05-19

Input				
Vehicle Parameters	Radius of curvature	R	[m]	105.00
	Total mass	m	[kg]	1742.00
	length	l	[m]	2.68
	Track width front	w1	[m]	1.52
	Track width rear	w2	[m]	1.51
	CoG height	h	[m]	0.50
	Roll center height front	h1	[m]	0.05
	Roll center height rear	h2	[m]	0.10
	% Weight in the front	wd	[%]	40.00
	Roll Stiffness	c_phi	[Nm/rad]	2190.00
	% Roll Stiffness front	c_phif	[%]	60.00
	static toe	st	[deg]	0.00
Magic tire parameters	Nominal load	Fzo	[N]	4000.00
	pCy1	pCy1	-	1.19
	pDy1	pDy1	-	-0.99
	pDy2	pDy2	-	0.15
	pEy1	pEy1	-	-1.00
	pEy2	pEy2	-	-0.54
	pKy1	pKy1	-	14.95
	pKy2	pKy2	-	2.13
	chi2	chi2	-	1.00
	chi3	chi3	-	1.00
	lmda_Cy	lmda_Cy	-	1.00
	lmda_muy	lmda_muy	-	1.00
	lmda_Ey	lmda_Ey	-	1.00
	lmda_Kya	lmda_Kya	-	1.00

Figure 3.8: Input Sheet

The input file containing the suspension and the tire parameters is saved for each configuration with a configuration name. The name of the input file is entered in a simple runscript developed in matlab as shown the figure 3.9

```

1 % Suspension Parameters Impact on Understeer
2 % Runscript
3 %-----
4 - clear
5 - clc
6 - x = xlsread('Config_name.xlsx');
7 - [parameters,Fz,dFz1,dFz2] = susp_understeer(x);

```

Figure 3.9: Runscript

The runscript initiates the function file *susp\_understeer* which is the source code. The code runs in the background and calculates the lateral acceleration, the load transfer, tire forces, the slip angles and the corresponding value for understeer gradient in the specified order as explained in the section 3.5. The process repeats with increase in the longitudinal velocity by  $0.1 \text{ m/s}$  until there exists no value for the slip angles. The flowchart for the process is given in Figure 3.10

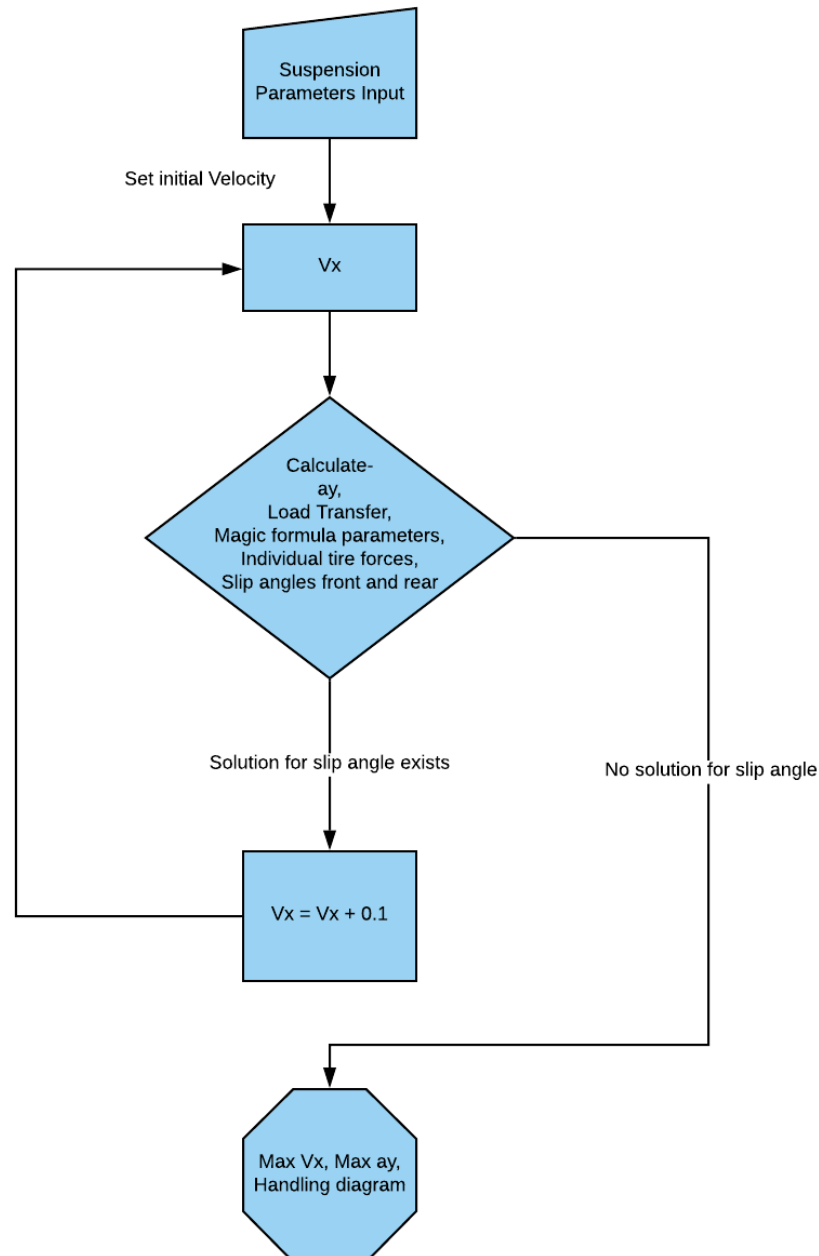


**Figure 3.10:** Flowchart of the code

### 3. Road-Holding and Handling Analysis

---

After reaching the velocity at which no solution exists for the equations, the code terminates and provides the value of maximum velocity that the vehicle with given configuration can travel around a corner and the corresponding maximum lateral acceleration experienced. Also, the handling diagram is displayed as an output that describes the vehicle's behaviour until the limit of adhesion. The output display is as shown in Figure 3.11 and 3.12.

```
Command Window
Max speed reached at 28.70 m/s
fx Max lateral acceleration = 7.84 m/s^2>> |
```

**Figure 3.11:** Velocity and Acceleration output

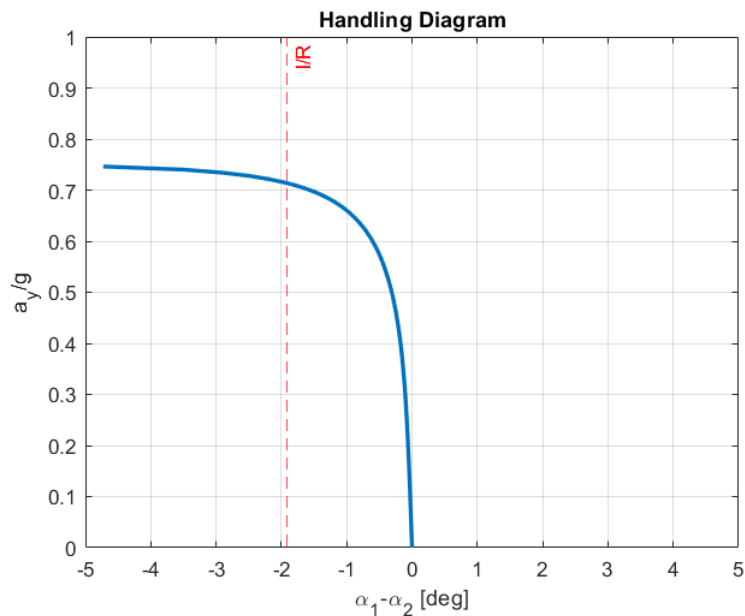


**Figure 3.12:** Handling diagram

# 4

## Validation and Results

The following section involves validation of the Model using different sets of data and variation of different parameters to understand their inter-dependency and their effect on the handling behaviour of the vehicle.

### 4.1 Validation of the Model

The validation of the Model is done using two sets of data; one set of data is obtained from an ÅF internal report and the other set of data is obtained from tests performed at the AstaZero test track. The comparison between the data sets with the Model data is done qualitatively by looking at the nature of variation rather than pinpointing each value quantitatively. The main reason for comparing the data qualitatively is that the tyre specifications of the used test vehicles at ÅF and AstaZero are unknown, whereas the tyre specifications and tyre model of the one used in building this Model have been mentioned in Appendix A.2. Furthermore, the Model does not include the suspension compliances, damping effects of bushings, distinction between roll stiffness distribution of anti-roll bar and springs, etc. which creates deviation of results from experimental data.

#### 4.1.1 Validation using ÅF Test Data

The setups used to run the Model are decided based on an internal report obtained from ÅF, as shown in the picture below:

Setup No.	Mass	Weight Distribution	Roll Stiffness	Roll Stiffness Distribution
	[kg]	(F/R) [%]	[Nm/deg]	(F/R) [%]
1. Gross Vehicle Weight	2038	54/46	2190	60/40
2. Design Weight	1742	61/39	2190	60/40
3. No Front ARB	1742	61/39	1237	30/70

**Figure 4.1:** Test cases obtained from internal report at ÅF

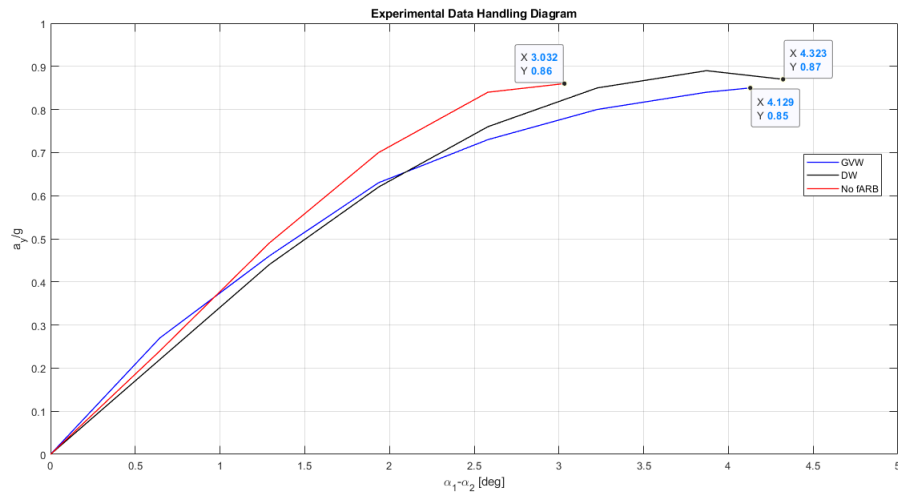
For the setups, there are two variations of Total Weight; the Gross Vehicle Weight of 2038 kg and the Design Weight of 1742 kg. Gross Vehicle Weight is the total weight of the vehicle including all the amenities, chassis, driver, passengers, cargo and all types of fluids. Design Weight is the total weight of the vehicle without the inclusion of any occupants, except the driver, one passenger alongside the driver and cargo.

#### 4. Validation and Results

As for Total Roll Stiffness, there are two variations: 2190 Nm/deg and 1237 Nm/deg. The reduction in the total roll stiffness in the second variation is due to no anti-roll bar in the front.

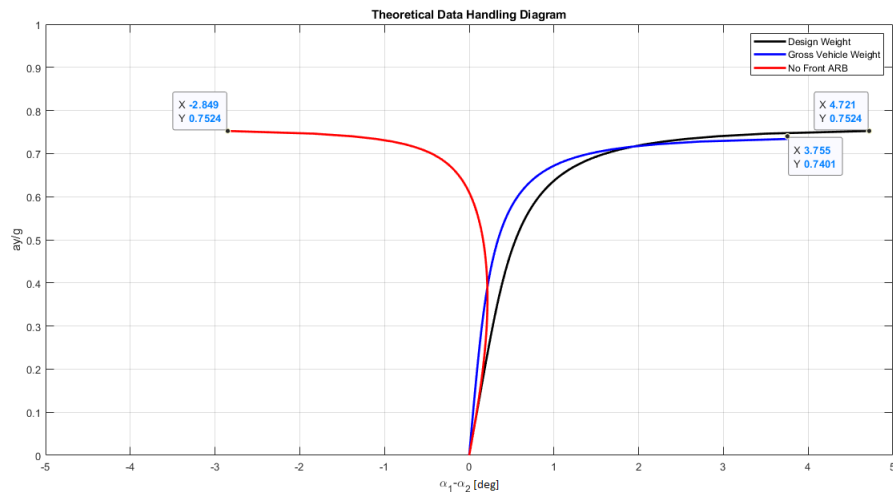
The Model is simulated for all the three setups and then the handling behaviour of the vehicle is compared with the data already available from ÅF.

Figure below shows the data of the three setups obtained from ÅF.



**Figure 4.2:** Handling Diagram for the 3 setups from ÅF test data

Plots of the same 3 setups of the theoretical Model are now shown below:



**Figure 4.3:** Handling Diagram of Theoretical Data from the Model

The table below summarizes the comparison of both the experimental data and the theoretical data.



	Experimental Data		Theoretical Data	
	$\alpha_1 - \alpha_2$ (deg)	$a_y/g$	$\alpha_1 - \alpha_2$ (deg)	$a_y/g$
Gross Vehicle Weight	4.129	0.85	3.755	0.7401
Design Weight	4.323	0.87	4.721	0.7524
No Front ARB	3.032	0.86	-2.849	0.7524

**Figure 4.4:** Comparison between ÅF Experimental and Theoretical data

#### 4.1.2 Validation using AstaZero Test Data

The second test data set to validate the Model is obtained from on-track steady state cornering test performed on the test track AstaZero (in Hålleröd, Sweden) in the same car as the ÅF test data, Saab 9-3. Below shown is the comparison between the AstaZero data and the Model data. Again, as mentioned before, the data is only compared qualitatively.

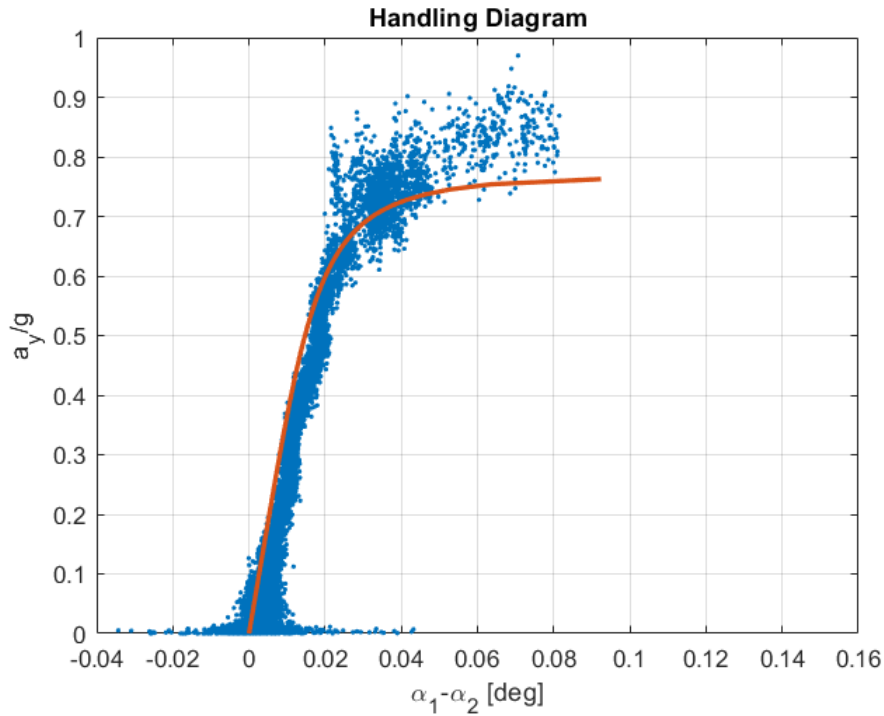


**Figure 4.5:** Data comparison between test data from AstaZero and the Model

## 4.2 Effect of change of centre of gravity location (or weight distribution) on handling of the vehicle

For this section the centre of gravity location will vary longitudinally and the rest of the setup stays the same. The setup used is the Design Weight setup, which has Mass = 1742 kg, Roll Stiffness = 2190 Nm/deg and Roll Stiffness Distribution = 60/40. The centre of gravity location variation effectively means changing the weight distribution as a percentage ratio of front to rear. The different weight distributions varied are 61/39, 54/46, 40/60.

Shown below are the three variations in handling behaviour due to the variations in centre of gravity location.

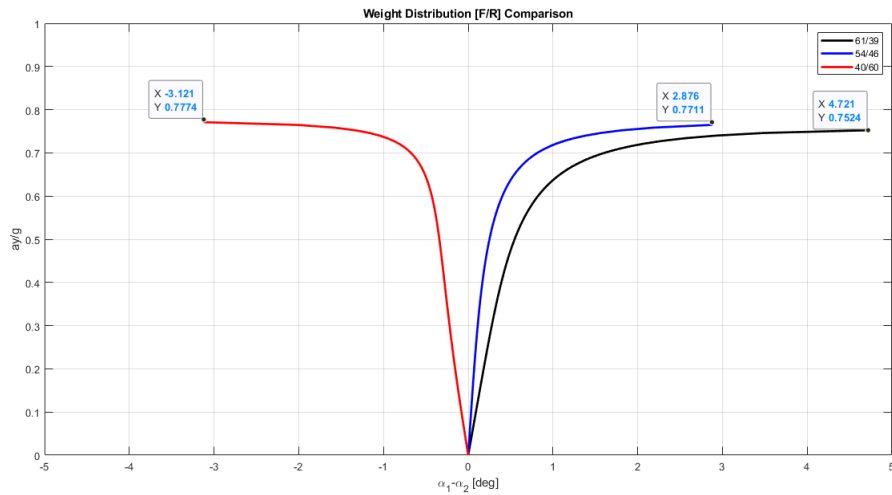


**Figure 4.6:** Handling Diagram comparison for the Weight Distribution variation

## 4.3 Effect of change of roll stiffness distribution on handling of the vehicle

Roll Stiffness Distribution is varied as a percentage ratio of front to rear as 60/40, 50/50 and 30/70. The base setup is kept the same throughout and only the roll stiffness distribution is changed.

Shown below is the combined Handling Diagram of the three variations.

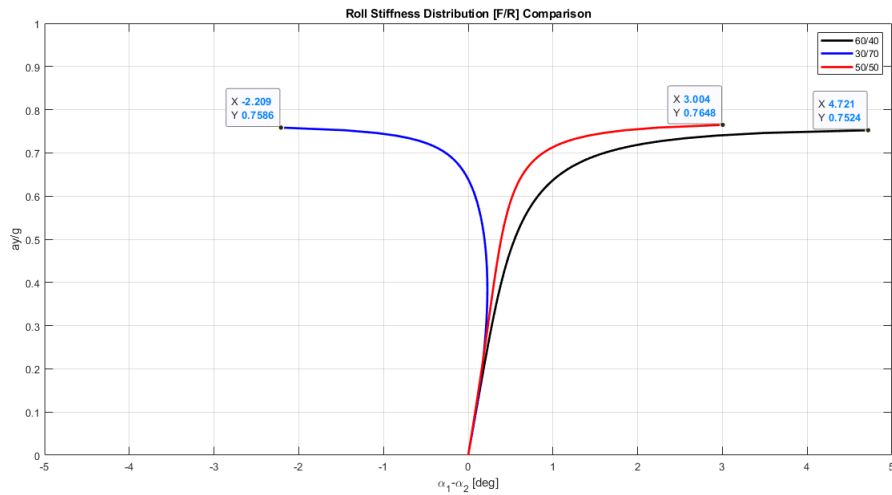


**Figure 4.7:** Handling Diagram comparison for the Roll Stiffness Distribution variation

#### 4.4 Effect of change of centre of gravity height on handling of the vehicle

To show the effect of change of height of centre of gravity on vehicle handling, the same Design Weight setup is used. The variations to the height of centre of gravity from ground are 0.5 metres, 0.7 metres and 0.3 metres. The combined Handling Diagram for all these three variations are shown below:

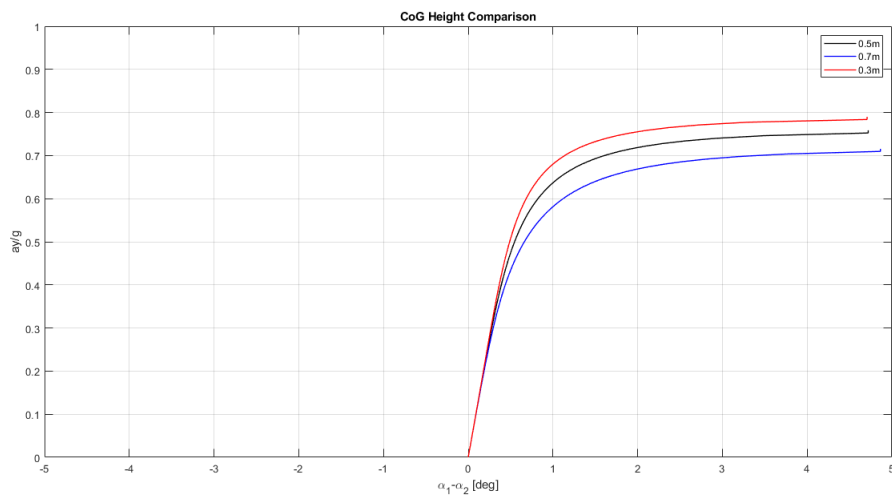


**Figure 4.8:** Handling Diagram for comparing the variation in Centre of Gravity Height

## 4.5 Effect of change of roll centre height on handling of the vehicle

To show the effect of roll centre height variation on handling behaviour, the same setup of Design Weight is used to start off. The different iterations of roll centre height variations in the front ( $h_1$ ) and rear ( $h_2$ ) are (0.045, 0.101) metres, (0,0) metres and (0.5,0.5) metres. Figures below show their effect on handling diagram:

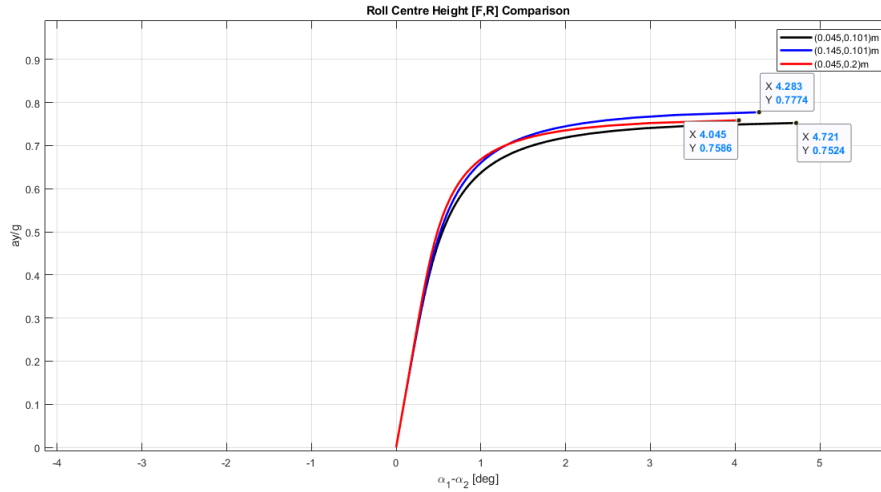


**Figure 4.9:** Handling Diagram for comparing the Roll Centre Height variation

# 5

## Discussions

The Model is built with an intention to be used by Design Engineers much early in the design process. The inputs to the Model are in the form of separate excel sheets of vehicle data and tyre data. The output of the Model can be in the form of maximum lateral acceleration achievable in Steady State Cornering for a given setup, a Handling Diagram to graphically and quantitatively show the understeer/oversteer behaviour and roll angle to understand the load transfer. There are a lot of practical parameters not included in the Model to keep it simple, such as the various suspension compliances, damping effects of bushings, roll stiffness distinction between the springs and anti-roll bar and inertia effects.

It is assumed that the difference between front outer and inner slip angles is very less in static condition, however, in practical situations static toe and ackermann steering are included in the wheel geometry. The Model includes the effect of ackermann steering and presents different values of front inner and outer slip angles, however, the effect of static toe does not show very sensitive results in this Model.

To test and validate the Model, first with the ÅF data, as shown in Figures 4.2 and 4.3, it is seen that the nature of the graph of Gross Vehicle Weight and Design Weight setups are similar, leaning increasingly towards understeer behaviour. Also, the lateral acceleration achieved in the Design Weight setup is more than that in the Gross Vehicle Weight setup in both sets of data. In the No Front ARB setup, the vehicle with ÅF data goes understeer and is the least amount of understeer compared to all three. However, the Model (theoretical data) shows understeer behaviour for low lateral acceleration levels and oversteer for high lateral accelerations. This is due to the fact that for lower lateral accelerations the vertical load on the front tyres is more so the vehicle tends to understeer. As the lateral acceleration increases, the load on rear outer increases rapidly and on rear inner decreases rapidly and after a certain point the rear outer has the maximum load out of the four tyres and the rear inner lifts up, which leads to an oversteer behaviour. Additionally, validation with the AstaZero Test data, as seen in Figure 4.5, shows that the Model generates handling behaviour very similar to the experimental data as the nature of both plots are almost overlapping.

For the handling behaviour comparison when weight distribution is being varied as shown in Figure 4.6, it can be seen that the plots suggest as we shift the weight distribution from front to rear, the vehicle handling shifts from understeer to oversteer. For the setup when the weight is more in the rear (40/60) the vehicle is more

oversteered (as discussed above), even though the roll stiffness is more in the front (60/40). As more roll stiffness attracts more load transfer the vehicle should have been understeered. This anomaly is understood more when vertical load data is looked upon, which shows that vertical load is more in the rear inner and outer tyres than the front tyres. So, even though the roll stiffness distribution is more in the front, the distribution is not effective enough to influence the handling behaviour in this case, which says that weight distribution has a bigger impact on handling behaviour, in this setup.

The variation in the handling behaviour of the vehicle when varying the roll stiffness distribution as shown in Figure 4.7 is similar in nature as is discussed when validating the Model with the ÅF test data above.

The effect of centre of gravity height variation on the handling behaviour as seen in Figure 4.8 can be understood better from the load transfer perspective. As centre of gravity height increases, the distance of centre of gravity from the roll axis also increases, which leads to higher roll and higher load transfer. As the load transfer increases, the amount of load on the outer tyre increases and the load on the inner tyre decreases, however, the increment in the outer tyre is lesser than the decrement in the inner tyre. This results in an effective lower lateral force generated by the axle, which reduces the lateral acceleration. Hence, as the centre of gravity height increases, the lateral acceleration decreases.

The effect of varying the front and rear roll centre heights as seen in Figure 4.9 can be explained in similar way as above. Increasing any of the two roll centre heights would lead to decreased distance of centre of gravity from the roll axis, which leads to lesser roll and lesser load transfer and ultimately, higher lateral accelerations.

# 6

## Conclusion

The objective of the thesis of building a tool to study the effect of different suspension and chassis parameters on handling behaviour of the vehicle is achieved for steady state manoeuvre. The tool presents the results in the form of a Handling Diagram, making it easier to directly interpret the handling behaviour, qualitatively and quantitatively. The tool is validated from the data obtained from an internal report at ÅF and AstaZero test data. However, due to time constraints the tool could not be made ready for the evaluation of dynamic manoeuvre and has been included in the Future Work to be done in a subsequent Thesis proposal.





# 7

## Future Work

### **Tool development for dynamic manoeuvre**

For transient and dynamic manoeuvre tool development, the additional effects of inertia, damping and the time lag between different compliances can be taken into consideration.

### **Roll stiffness distribution split**

The roll stiffness of the vehicle can be further split into contributions from the springs and the anti-roll bar, including the studying of spring rate and motion ratio of both, which will help in understanding the effect of both on vehicle handling behaviour in detail. It is possible that by achieving the "Roll stiffness distribution split", the anomaly observed in the Validation with ÅF test data for No Front ARB setup (section 4.1.1) will be reduced.



# Bibliography

- [1] R.T Bundorf, R.L Leffert, "The Cornering Compliance Concept for Description of Vehicle Directional Control Properties", SAE paper 760713
- [2] Walter Bergman, "The basic Nature of Vehicle Understeer-Oversteer", SAE paper 650085
- [3] Douglas L. Milliken William F. Milliken. "Race Car Vehicle Dynamics". SAE International, 1994. ISBN:1-56091-526-9 978-1-56091-526-3.
- [4] Hans B. Pacejka & Egbert Bakker (1992) "The Magic Formula Tyre Model", Vehicle System Dynamics, 21:S1, 1-18
- [5] Hans B. Pacejka, "Tire and Vehicle Dynamics", ISBN:9780080543338
- [6] John Weldin, Lars-Runo Tillback, Olof Bane (1992), "Combining Properties for Driving Pleasure and Driving Safety: A Challenge for the Chassis Engineer", Future Transportation Technology Conference and Exposition Costa Mesa, California, SAE paper 921595
- [7] Damrongrit (Neng) Piyabongkarn, Rajesh Rajamani, John A. Grogg, and Jae Y. Lew, (2009), "Development and Experimental Evaluation of a Slip Angle Estimator for Vehicle Stability Control", IEEE Transactions on Control Systems Technology, Vol. 17
- [8] Matthijs Klomp,(2007) "On Drive Force Distribution and Road Vehicle Handling - A Study of Understeer and Lateral Grip", Licentiate Thesis, Chalmers University of Technology
- [9] Bengt Jacobson, "Vehicle Dynamics Compendium" for Course MMF062. 2017.
- [10] Mathias Lidberg, Lecture notes for TME102- Advanced Vehicle Dynamics, Chalmers University of Technology
- [11] Mathworks, Tire Road Interaction (Magic Formula), Magic formula coefficients for Typical road conditions, <https://se.mathworks.com/help/physmod/sdl/ref/tireroadinteractionmagicformula.html>



# A

## Appendix 1

### A.1 Vehicle Data

Parameter	Value	Unit	Description
<b>m</b>	1675	kg	mass
<b>l</b>	2.675	m	wheelbase
<b>a1</b>	1.07	m	Distance of front axle from cog
<b>a2</b>	1.605	m	Distance of rear axle from cog
<b>w1</b>	1.517	m	front track width
<b>w2</b>	1.505	m	rear track width
<b>h</b>	0.5	m	Distance of center of gravity from the ground
<b>h1</b>	0.045	m	Roll center height on the front axle
<b>h2</b>	0.101	m	Roll center height on the rear axle
<b>c_phi1</b>	16.22	N/rad	Roll stiffness front
<b>c_phi2</b>	7.837	N/rad	Roll stiffness rear

Figure A.1: Vehicle Data

### A.2 Tire Data

Magic tire parameters	Nominal load	Fzo	[N]	4000.00
	pCy1	pCy1	-	1.19
	pDy1	pDy1	-	-0.99
	pDy2	pDy2	-	0.15
	pEy1	pEy1	-	-1.00
	pEy2	pEy2	-	-0.54
	pKy1	pKy1	-	14.95
	pKy2	pKy2	-	2.13
	chi2	chi2	-	1.00
	chi3	chi3	-	1.00
	lmda_Cy	lmda_Cy	-	1.00
	lmda_muy	lmda_muy	-	1.00
	lmda_Ey	lmda_Ey	-	1.00
	lmda_Kya	lmda_Kya	-	1.00

[5]

Figure A.2: Tire Data

## A.3 MATLAB Code

### Runscript

```
1 % Suspension Parameters Impact on Understeer
2 % Runscript
3
4 clear
5 clc
6 x = xlsread('Config1.xlsx');
7 [parameters,Fz,dFz1,dFz2] = susp_understeer(x);
```

### Code

```
1 function [parameters,Fz,dFz1,dFz2] = susp_understeer(x)
2
3 % Input Data%
4
5 R = x(1);
6 m = x(2);
7 l = x(3);
8 w1 = x(4);
9 w2 = x(5);
10 h = x(6);
11 h1 = x(7);
12 h2 = x(8);
13 wd = x(9)/100;
14 c_phi = x(10);
15 c_phif = x(11)/100;
16 sr = x(12);
17 k_delta = x(13);
18
19 % Magic Tire Parameters
20
21 Fzo = x(14);
22
23
24 pCy1 = x(15);
25 pDy1 = x(16);
26 pDy2 = x(17);
27 pEy1 = x(18);
28 pEy2 = x(19);
29 pKy1 = x(20);
30 pKy2 = x(21);
31 chi2 = x(22);
```

```

32 % chi3 = x(23);
33
34 lmda_Cy = x(24);
35 % lmda_muy = x(25);
36 % lmda_Ey = x(26);
37 lmda_Kya = x(27);
38
39
40 % Calculations
41
42 g = 9.81;
43 a1 = (1-wd)*l;
44 a2 = wd*l;
45 hr = h - (((h2-h1)*a1/l)+ h1);
46 s1 = w1/2;
47 s2 = w2/2;
48
49 Fz1 = m*g*(1-a1)/l;      % Front axle weight [N]
50 Fz2 = m*g*(1-a2)/l;      % Rear axle weight [N]
51
52 c_phi1 = c_phi*c_phif*57.3;
53 c_phi2 = c_phi*(1-c_phif)*57.3;
54
55
56 % Logical Sequence %
57
58 exit = 1;
59 t = 1;
60 vx = 0.1;
61 w0 = [0,0,0,0,0,0,0,0,0,0,0,0];
62 ay(t) = zeros(t);
63
64
65 while exit > 0
66     ay(t) = vx^2/R;
67     Fy = m*ay(t);      % Total lateral force [N]
68     Fy1 = Fy*(1-a1)/l; % Front axle lateral force [N]
69     Fy2 = Fy*(1-a2)/l; % Rear axle lateral force [N]
70
71
72 % Load Transfer %
73
74 dFz1(t) = (1/(2*s1))*((c_phi1*hr/(c_phi1+c_phi2- m*hr*g))+((1
    -a1)*h1/l))) *m*ay(t); % Load transfer front [N]
75 dFz2(t) = (1/(2*s2))*((c_phi2*hr/(c_phi1+c_phi2- m*hr*g))+((1
    -a2)*h2/l))) *m*ay(t); % Load transfer rear [N]

```

```
76
77 Fz1o = Fz1/2 + dFz1(t);      % Front outer tyre weight [N]
78 Fz2o = Fz2/2 + dFz2(t);      % Rear outer tyre weight [N]
79 Fz1i = Fz1/2 - dFz1(t);      % Front inner tyre weight [N]
80 Fz2i = Fz2/2 - dFz2(t);      % Rear inner tyre weight [N]
81
82 Fz(t,:) = [Fz1o,Fz2o,Fz1i,Fz2i];
83
84
85 % Tyre Model %
86
87     dfz = zeros(1,4);
88
89 for i = 1:4
90     dfz(i) = Fz(t,i)/Fzo;
91 end
92
93
94     By = zeros(1,4);
95     Cy = pCy1*lmda_Cy;
96     Dy = zeros(1,4);
97     Ey = zeros(1,4);
98     Ky = zeros(1,4);
99     muy = zeros(1,4);
100
101
102 for i=1:4
103     muy(i) = (pDy1 + pDy2*dfz(i));
104     Dy(i) = muy(i)*Fz(t,i)*chi2;
105     Ey(i) = (pEy1 + pEy2*dfz(i));
106     Ky(i) = (pKy1*Fzo*sin(2*atan(Fz(t,i)/(pKy2*Fzo))))*
        lmda_Kya;
107     By(i) = Ky(i)/(Cy*Dy(i));
108 end
109
110 f1 = @(a1i,a1o,a2i,a2o,drw,dsw,vy,r,Fy1i,Fy1o,Fy2i,Fy2o) a1i
    - (drw - (vy + a1*r)/(vx - s1*r));
111 f2 = @(a1i,a1o,a2i,a2o,drw,dsw,vy,r,Fy1i,Fy1o,Fy2i,Fy2o) a1o
    - (drw - (vy + a1*r)/(vx + s1*r));
112 f3 = @(a1i,a1o,a2i,a2o,drw,dsw,vy,r,Fy1i,Fy1o,Fy2i,Fy2o) a2i
    + (vy - a2*r)/(vx - s2*r);
113 f4 = @(a1i,a1o,a2i,a2o,drw,dsw,vy,r,Fy1i,Fy1o,Fy2i,Fy2o) a2o
    + (vy - a2*r)/(vx + s2*r);
114 f5 = @(a1i,a1o,a2i,a2o,drw,dsw,vy,r,Fy1i,Fy1o,Fy2i,Fy2o) 1/R
    + (a1i+a1o)/2 - (a2i+a2o)/2 - drw;
```



```

115 f6 = @(a1i,a1o,a2i,a2o,drw,dsw,vy,r,Fy1i,Fy1o,Fy2i,Fy2o)
      Fy1o - Dy(1)*sin(Cy*atan(By(1)*a1o - Ey(1)*(By(1)*a1o -
      atan(By(1)*a1o)))));
116 f7 = @(a1i,a1o,a2i,a2o,drw,dsw,vy,r,Fy1i,Fy1o,Fy2i,Fy2o)
      Fy2o - Dy(2)*sin(Cy*atan(By(2)*a2o - Ey(2)*(By(2)*a2o -
      atan(By(2)*a2o)))));
117 f8 = @(a1i,a1o,a2i,a2o,drw,dsw,vy,r,Fy1i,Fy1o,Fy2i,Fy2o)
      Fy1i - Dy(3)*sin(Cy*atan(By(3)*a1i - Ey(3)*(By(3)*a1i -
      atan(By(3)*a1i)))));
118 f9 = @(a1i,a1o,a2i,a2o,drw,dsw,vy,r,Fy1i,Fy1o,Fy2i,Fy2o)
      Fy2i - Dy(4)*sin(Cy*atan(By(4)*a2i - Ey(4)*(By(4)*a2i -
      atan(By(4)*a2i)))));
119 f10 = @(a1i,a1o,a2i,a2o,drw,dsw,vy,r,Fy1i,Fy1o,Fy2i,Fy2o) Dy
      (1)*sin(Cy*atan(By(1)*a1o - Ey(1)*(By(1)*a1o - atan(By(1)
      *a1o)))) + Dy(3)*sin(Cy*atan(By(3)*a1i - Ey(3)*(By(3)*a1i
      - atan(By(3)*a1i)))) - Fy1;
120 f11 = @(a1i,a1o,a2i,a2o,drw,dsw,vy,r,Fy1i,Fy1o,Fy2i,Fy2o) Dy
      (2)*sin(Cy*atan(By(2)*a2o - Ey(2)*(By(2)*a2o - atan(By(2)
      *a2o)))) + Dy(4)*sin(Cy*atan(By(4)*a2i - Ey(4)*(By(4)*a2i
      - atan(By(4)*a2i)))) - Fy2;
121 f12 = @(a1i,a1o,a2i,a2o,drw,dsw,vy,r,Fy1i,Fy1o,Fy2i,Fy2o) sr
      *(k_delta*(dsw - drw*sr))-(Fy1o+Fy1i)*0.04;
122
123
124 % The SysEqn solves the system of equations with the 12
      unknowns.
125
126 SysEqn = @(w) [f1(w(1),w(2),w(3),w(4),w(5),w(6),w(7),w
      (8),w(9),w(10),w(11),w(12));
127      f2(w(1),w(2),w(3),w(4),w(5),w(6),w(7),w(8),w(9),w
      (10),w(11),w(12));
128      f3(w(1),w(2),w(3),w(4),w(5),w(6),w(7),w(8),w(9),w
      (10),w(11),w(12));
129      f4(w(1),w(2),w(3),w(4),w(5),w(6),w(7),w(8),w(9),w
      (10),w(11),w(12));
130      f5(w(1),w(2),w(3),w(4),w(5),w(6),w(7),w(8),w(9),w
      (10),w(11),w(12));
131      f6(w(1),w(2),w(3),w(4),w(5),w(6),w(7),w(8),w(9),w
      (10),w(11),w(12));
132      f7(w(1),w(2),w(3),w(4),w(5),w(6),w(7),w(8),w(9),w
      (10),w(11),w(12));
133      f8(w(1),w(2),w(3),w(4),w(5),w(6),w(7),w(8),w(9),w
      (10),w(11),w(12));
134      f9(w(1),w(2),w(3),w(4),w(5),w(6),w(7),w(8),w(9),w
      (10),w(11),w(12));

```

```

135         f10(w(1),w(2),w(3),w(4),w(5),w(6),w(7),w(8),w(9),w
136             (10),w(11),w(12));
137         f11(w(1),w(2),w(3),w(4),w(5),w(6),w(7),w(8),w(9),w
138             (10),w(11),w(12));
139         f12(w(1),w(2),w(3),w(4),w(5),w(6),w(7),w(8),w(9),w
140             (10),w(11),w(12));
141
142     options = optimset('Display','off');
143     [sol(t,:),~,exitflag] = fsolve(SysEqn,w0,options);
144     exit = exitflag;
145
146     if (exit > 0)
147         vx = vx+0.1;
148         w0 = sol(t,:);
149         t = t+1;
150     else
151         sol(t,:) = []; % Deleteing the last row
152         ay(t) = []; % Deleteing the last row
153         Fz(t,:) = []; % Deleteing the last row
154         max_acc = ay(t-1);
155         max_vx = vx -0.1;
156         fprintf('Maximum acc = %d\n',max_acc);
157         fprintf('Maximum vel = %d\n',max_vx);
158     end
159 end
160
161 dsw = sol(:,6)';
162 figure(1)
163 plot((dsw/sr - l/R)*57.3,ay/g,'LineWidth',2)
164 xline(-l/R*57.3,'-r',{ 'l/R' });
165 grid on
166 xlabel('\alpha_1-\alpha_2 [deg]')
167 ylabel('a_y/g')
168 xlim([-5 5])
169 ylim([0 1])
170 title('Handling Diagram')
171
172 parameters = sol;

```

## A.4 User Manual

This section describes the steps to be followed for the working of the tool.

- Ensure that the function file, the runscript and the Input file are all in the same location.

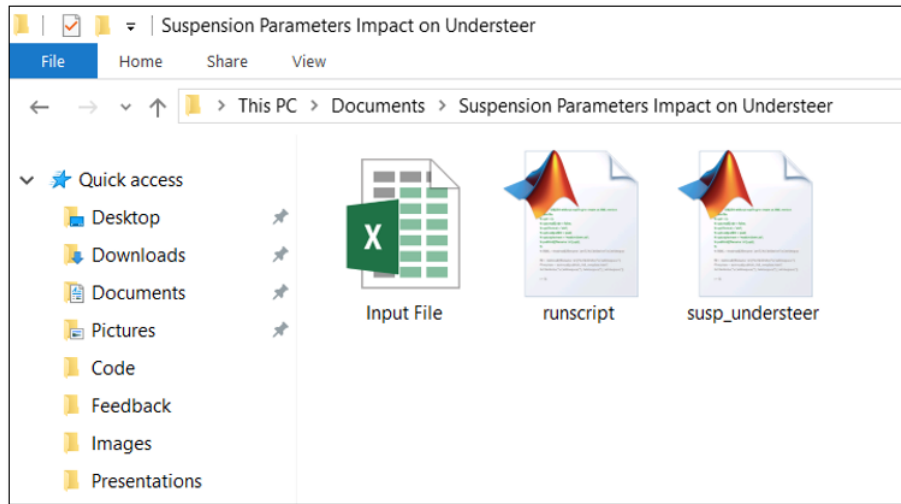


Figure A.3: Step1

- Open the Input file
- Enter the values for the parameters
- Enter the configuration name
- Use 'Save As' to save the the excel file in the same name as the configuration

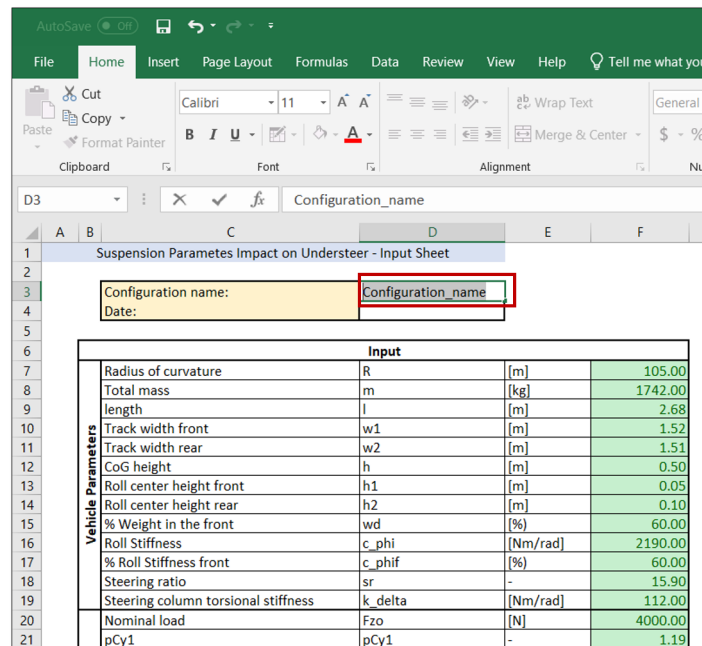
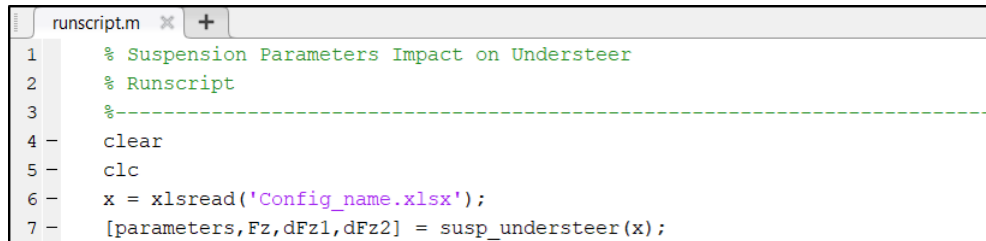


Figure A.4: Step2

- Open 'runscript.m'
- In the line 6 of the code, replace 'Config1.xlsx' with the name of your excel input file '*Configuration\_name.xlsx*'
- Press Run button



```
runscript.m  x  +
1  % Suspension Parameters Impact on Understeer
2  % Runscript
3  %-----
4  clear
5  clc
6  x = xlsread('Config_name.xlsx');
7  [parameters,Fz,dFz1,dFz2] = susp_understeer(x);
```

Figure A.5: Step3

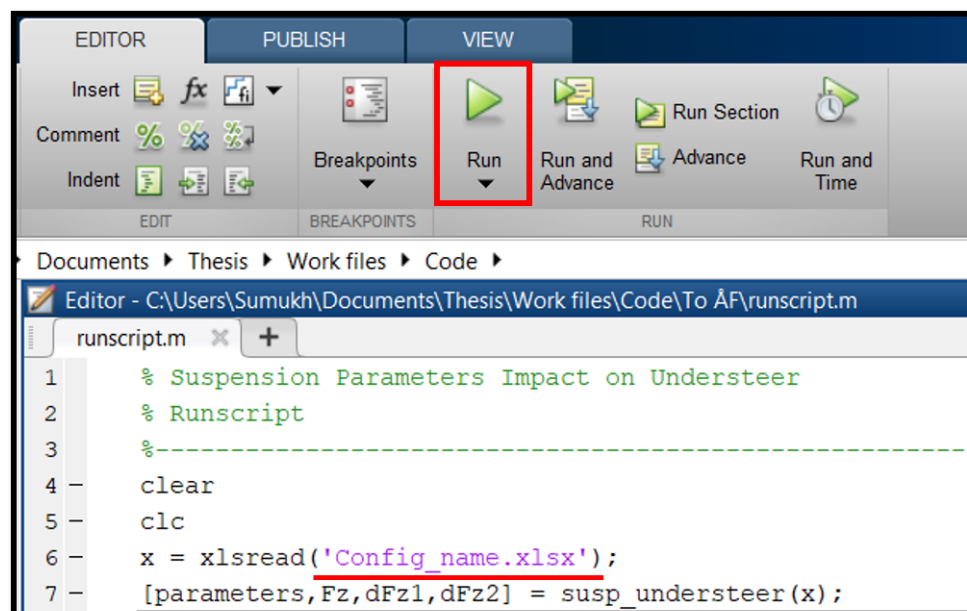


Figure A.6: Step4